On the anomaly of susceptibility for quantum spin systems

相場, 信孝

Doctoral Thesis

On the anomaly of susceptibility for quantum spin systems

Nobutaka Aiba

Department of Physics, Kyushu University, Fukuoka, 819-0395, Japan

Abstract

In this thesis, we propose a novel method of evaluating an anomaly by investigating the magnetic susceptibility χ and the fourth derivative A of the energy with respect to magnetization. The term 'anomaly' means a divergence in the thermodynamic limit. This anomaly usually marks a phase transition. Researchers have studied the anomaly of the magnetic susceptibility from exact solutions. However, few investigations of high-order differentials such as A have been carried out. We show that the method observing the anomaly by χ and A is appropriate for the analysis of the phase transition, compared with the method using the magnetic susceptibility χ alone. The introduction of A resolves the issue of whether the high-order differential of energy diverges.

As an example, we apply this method to the $S = 1/2$ XXZ antiferromagnetic chain, which shows a ferromagnetic phase for $\Delta \leq -1$, Tomonaga–Luttinger (TL) phase for $-1 < \Delta \leq 1$, and antiferromagnetic phase for $\Delta > 1$. Δ is an anisotropic parameter with the z component of the XXZ antiferromagnetic chain. The lowest energy of the chain is calculated by numerical diagonalization. Subsequently, we analyze the anomalies of χ and A to observe the phase transition.

The results demonstrate that an anomaly of χ^{-1} at zero magnetization exists under $\Delta > 1$, while A at zero magnetization shows an anomaly for $\Delta > 1/2$. Hence, the anomaly of A is easier to observe than that of χ. We then consider the anomaly from the perspective of the scaling dimension which indicates the critical phenomena. The scaling dimension of the chain is subject to the parameter Δ. For $\Delta = 1$, the scaling dimension changes from irrelevant to relevant for $U(1)$ symmetry. This change of the scaling dimension means the phase transition corresponding to the Kosterlitz–Thouless (KT) transition. In contrast, for $-1 < \Delta \leq 1$ region that shows Tomonaga–Luttinger (TL) phase, the scaling dimension is irrelevant. For $\Delta = 2$ region that shows the antiferromagnetic phase, the scaling dimension x_T is relevant in $\Delta > 1$. Thus, we conclude that the anomaly of A at $1/2 < \Delta < 1$ is different from that of A at $\Delta = 1$ and does not indicate the phase transition. Moreover, we reveal that TL phase is divided into two phases with a $\Delta = 1/2$ boundary by the behavior of A. We refer to $-1 < \Delta < 1/2$ as TL phase (I) and $1/2 < \Delta \leq 1$ as TL phase (II).

These findings indicate that the method using A is better than that using χ for analyzing critical phenomena with phase transitions.

Contents

Chapter 1

Introduction

1.1 Condensed matter and spin

In condensed matter physics, phase transitions and their corresponding energy gaps are important research subjects. Researching these gaps is necessary for studying the behavior of quantum spin systems. Bethe showed that an $S = 1/2$ antiferromagnetic Heisenberg chain had the characteristic of the absence of a gap [1]. In addition, it was confirmed that the correlation function for the system decreases with a power low. Later, Haldane argued the difference between half-odd-integer and integer spin antiferromagnet chains [2]. For the integer spin case, Haldane showed that the antiferromagnetic Heisenberg chain have a gap and the correlation function is exponentially decreased.

Many researchers have observed the energy gap via the magnetization curve as a function of the magnetic field. The magnetic field at zero magnetization is equal to the magnitude of the gap. However, the method of observing the gap via the magnetization curve is not appropriate for deciding whether a spin system is gapless or gapped in numerical calculation; it is difficult to distinguish a gapless system from one with a very small energy gap [3]. Hence, Sakai and Nakano [4, 5, 6, 7] proposed a method for distinguishing a gapless system from a gapped system. In the next section, we introduce Sakai and Nakano's method.

1.2 Anomaly of magnetic susceptibility

In this section, we review Sakai and Nakano's work [4], which shows a method for distinguishing a gapless from a gapped system and an anomaly of magnetic susceptibility. The term 'anomaly' means that the magnetic susceptibility diverges in the thermodynamic limit.

First, they focus on the spin $S = 1/2$ square lattice antiferromagnetic Heisenberg model in two dimensional systems. The Hamiltonian of the model is given by

$$\hat{\mathscr{H}} = J_1 \sum_{\langle i,j \rangle} (\hat{S}_i^x \hat{S}_j^x + \hat{S}_i^y \hat{S}_j^y + \hat{S}_i^z \hat{S}_j^z) + J_2 \sum_{\langle k,l \rangle} (\hat{S}_k^x \hat{S}_l^x + \hat{S}_k^y \hat{S}_l^y + \hat{S}_k^z \hat{S}_l^z), \quad (1.1)$$

where J_1, J_2 are an exchange interaction, $\hat{S}_i, \hat{S}_j, \hat{S}_k, \hat{S}_l$ are the spin operator, and $\langle i, j \rangle$ and $\langle k, l \rangle$ indicate the nearest neighbor pairs on the lattice. Figure 1.1 shows the model (1.1). In $J_1 \gg J_2$, neighboring spins form pair, which indicates a spin-singlet state (Fig. 1.2). Subsequently, the lowest energy $E(N, M)$ and magnetization M of the model (1.1) are defined as

$$\hat{\mathscr{H}} |\phi\rangle = E(N, M) |\phi\rangle ,$$
$$\sum_{j=1}^{N} \hat{S}_j^z |\phi\rangle = M |\phi\rangle ,$$

where N is the system size, M is a magnetization, $\hat{S}_j^z$ is the jth spin operator in z direction, and $|\phi\rangle$ is the eigenstate. We note that $|\phi\rangle$ is a simultaneous eigenstate of $\hat{\mathscr{H}}$ and $\sum_j \hat{S}_j^z$. To calculate the lowest energy, a numerical diagonalization method is used under a periodic boundary condition. The interaction to the external magnetic field h is

$$\hat{\mathscr{H}}_z = -h \sum_{j=1}^{N} \hat{S}_j^z. \quad (1.2)$$

In the thermodynamic limit ($N \to \infty$), the lowest energy of $\hat{\mathscr{H}}$ per site, $\epsilon(m)$, is defined as

$$\lim_{N \to \infty} \frac{E(N, M)}{N} = \epsilon(m), \quad (1.3)$$

where $m = M/M_s$ is a magnetization normalized and $M_s = SN$ is a saturation magnetization which means the magnetization of the state where all the spins are aligned in the z direction. They then consider $\epsilon''(m)$ and $\epsilon'(m)$. When $\epsilon(m)$ is analytic, the spin excitation energy $E(N, M + 1) - E(N, M)$ becomes

$$\frac{1}{N}(E(N, M + 1) - E(N, M)) \simeq \epsilon \left(m + \frac{1}{NS} \right) - \epsilon(m). \quad (1.4)$$

From Taylor expansion of $\epsilon \left(m + \frac{1}{NS}\right)$, Eq. (1.4) is written as

$$E(N, M + 1) - E(N, M) \simeq \frac{1}{S}\epsilon'(m) + \frac{1}{2NS^2}\epsilon''(m) + \cdots. \quad (1.5)$$

Similarly, the spin excitation energy $E(N, M) - E(N, M-1)$ becomes

$$E(N, M) - E(N, M-1) \simeq \frac{1}{S}\epsilon'(m) - \frac{1}{2NS^2}\epsilon''(m) + \cdots. \tag{1.6}$$

From Eq. (1.5) and Eq. (1.6), $\epsilon''(m)$ is given by

$$(E(N, M+1) - E(N, M)) - (E(N, M) - E(N, M-1)) \simeq \frac{1}{NS^2}\epsilon''(m). \tag{1.7}$$

This indicates that $\epsilon''(m)$ is represented by the difference of energies. By minimizing the energy of total Hamiltonian including Eq. (1.1) and Eq. (1.2), $\epsilon'(m)$ is written as

$$\begin{aligned} &\frac{\partial}{\partial m}\left(\frac{E(N, M)}{N} - h\frac{M}{N}\right) = 0 \\ &h = \frac{\epsilon'(m)}{S}. \end{aligned} \tag{1.8}$$

As $\epsilon(m)$ is assumed to be analytic, $\epsilon'(0)$ becomes zero. Conversely, assuming that $\epsilon(m)$ is not analytic, $\epsilon'(0)$ becomes finite.

The derivative of m with respect to h is defined as

$$\chi \equiv \frac{dm}{dh} = \frac{S}{\epsilon''(m)}, \tag{1.9}$$

where χ is a magnetic susceptibility. In particular, in the case of $m = 0$, Eq. (1.7) is written as follows

$$2\Delta_{NS} \simeq \frac{1}{NS^2}\epsilon''(0), \tag{1.10}$$

where $\Delta_{NS} = E(N, 1) - E(N, 0)$ is the spin energy gap. When $\chi(m = 0) = 0$, $\epsilon''(m = 0)$ is infinite in the thermodynamic limit. In contrast, when $\chi(m = 0) \neq 0$, $\epsilon''(m = 0) = 0$ in the thermodynamic limit. In the thermodynamic limit, the relation between χ and Δ_{NS} is

$$\begin{cases} \lim_{N\to\infty} \chi(m = 0) = 0 & (1.11) \\ \qquad \Rightarrow \Delta_{NS} = \text{finite} \quad \text{(gapped)}, & \\ \lim_{N\to\infty} \chi(m = 0) \neq 0 & (1.12) \\ \qquad \Rightarrow \Delta_{NS} = 0 \quad \text{(gapless)}. & \end{cases}$$

This indicates whether the spin systems is gapless or gapped from the numerical results of χ.

The model (1.1) is gapless for $\alpha > \alpha_c$ where $\alpha_c = 0.52337(3)$ and $\alpha = J_1/J_2$, while this model is gapped for $\alpha < \alpha_c$ [8]. They then calculate χ for the model (1.1). Figure 1.3 shows the magnetization dependence of χ for the model (1.1). Figure 1.3(a) shows that the curve is smooth and $\chi \neq 0$ at $m = 0$ for $\alpha = J_2/J_1 = 1$. Conversely, Fig. 1.3(b) shows that $\chi = 0$ at $m = 0$ for $\alpha = J_2/J_1 = 0.2$, and χ seems to diverge near $m = 0$ in the thermodynamic limit. The divergence near $m = 0$ in Fig. 1.3(b) means the anomaly of magnetic susceptibility. Figure 1.4 shows the $1/N$ dependence of χ at $m = 0$. Figure 1.4(a) indicates that χ at $m = 0$ becomes finite in the thermodynamic limit. In contrast, Fig. 1.4(b) indicates that χ at $m = 0$ becomes zero in the thermodynamic limit. Thus, the numerical results of χ demonstrate that the model (1.1) is gapless for $\alpha = 1$ and is gapped for $\alpha = 0.2$.

These results indicate that they propose a method for distinguishing a gapless system from a gapped system by using magnetic susceptibility χ. We focus on the anomaly of magnetic susceptibility χ near zero magnetization in Fig. 1.3(b). The term ‘anomaly’ refers to a divergence in the thermodynamic limit. This anomaly usually exhibits a phase transition.

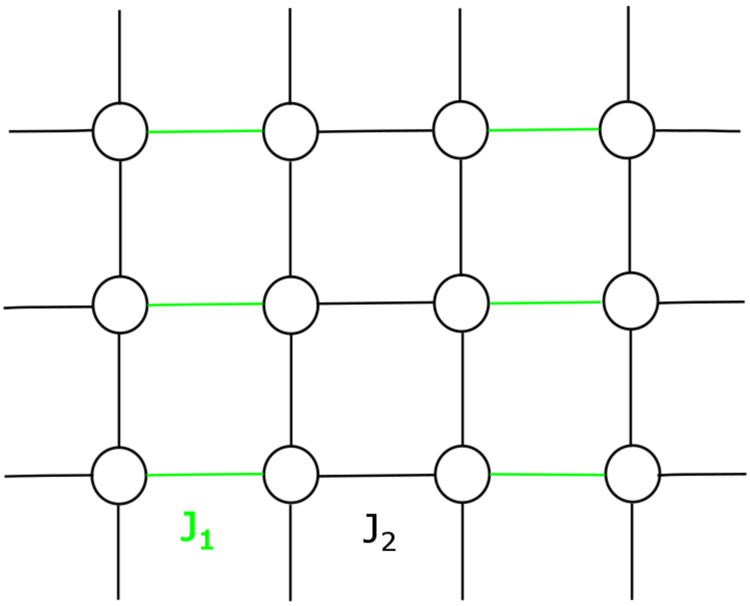

Fig. 1.1: Square lattice antiferromagnetic Heisenberg model. The solid green line and black line are the exchange interaction J_1 and the exchange interaction J_2 of the model (1.1).

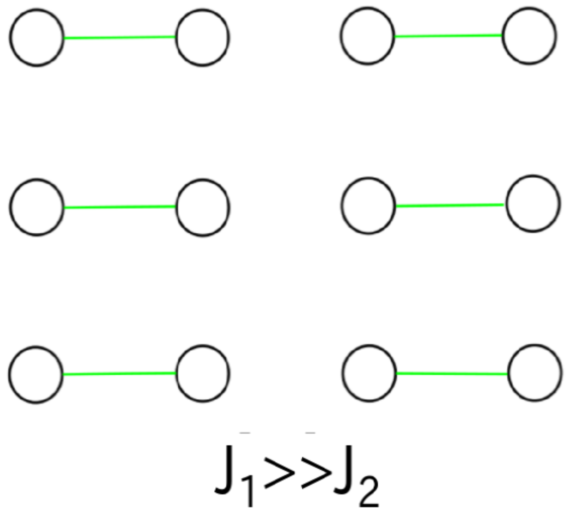

Fig. 1.2: Spin-singlet state that neighboring spins form pair when the exchange interactions $J_1 \gg J_2$ of the model (1.1).

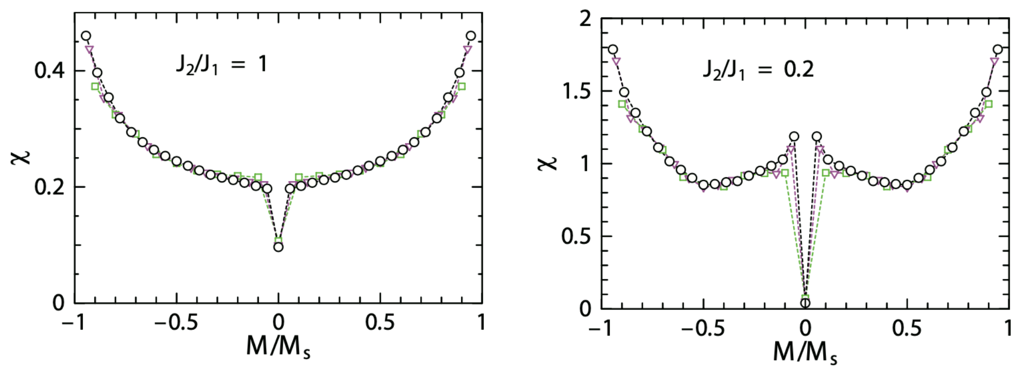

(a) gapless **(b)** gapped

Fig. 1.3: Magnetization $M/M_s = m$ dependence of the magnetic susceptibility χ for $S = 1/2$ square lattice antiferromagnetic Heisenberg model (1.1) reproduced from [4]. Panel (a) indicates that χ at $m = 0$ is finite. Thus, the system for a ratio of exchange interactions $J_2/J_1 = 1$ is gapless from Eq. (1.12). Conversely, panel (b) indicates that χ at $m = 0$ is 0 and the system for the ratio $J_2/J_1 = 0.2$ is gapped from Eq. (1.11).

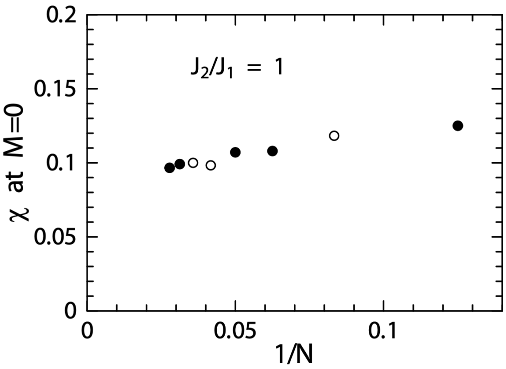

(a) gapless

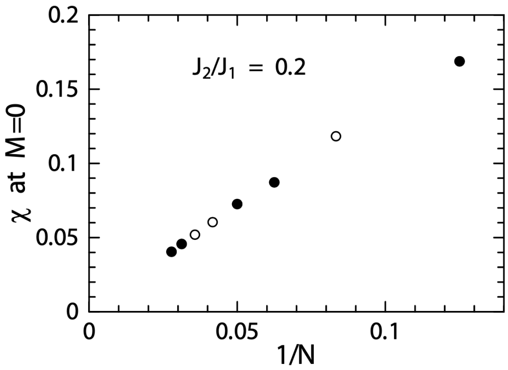

(b) gapped

Fig. 1.4: $1/N$ dependence of χ at magnetization $m = M/M_s = 0$ of $S = 1/2$ square lattice antiferromagnetic Heisenberg model (1.1) reproduced from [4]. Panel (a) shows that χ at $m = 0$ is finite in $N \to \infty$ and the system is gapless from Eq. (1.12). Panel (b) shows that χ at $m = 0$ is 0 in $N \to \infty$. Thus, the system is gapped from Eq. (1.11).

1.3 Purpose of research

From previous work of Nakano and Sakai, this study discusses a novel approach of evaluating an anomaly by studying the magnetic susceptibility χ and the fourth derivative A of the energy with respect to magnetization. The derivative of energy with respect to magnetization is introduced because it has a smaller error than that with respect to magnetic field. The aim of this study is analyzing the phase transition by using high-order differentials such as A. As a test case, in a numerical calculation, we apply this theory to the $S = 1/2$ XXZ antiferromagnetic chain, which shows a ferromagnetic phase for $\Delta \leq -1$, Tomonaga–Luttinger (TL) phase for $-1 < \Delta \leq 1$, and antiferromagnetic phase for $\Delta > 1$. Here, Δ denotes an anisotropic parameter associated with the z component of the XXZ antiferromagnetic chain. We show that χ and A derived from Bethe ansatz and conformal field theory are consistent with numerical results.

1.4 Organization of this thesis

This thesis is organized as follows: In the next chapter, we present some reviews of one-dimensional quantum spin systems. In Chapter 3, we introduce some physical quantities which are magnetic susceptibility χ and the fourth derivative A of the lowest energy with respect to magnetization. In addition, we introduce a conformal field theory and derive χ and A from the conformal field theory describing the low-energy behavior of the $S = 1/2$ XXZ chain. In Chapter 4, our numerical results are presented for the $S = 1/2$ XXZ antiferromagnetic chain. These results suggest that χ and A have an anomaly in the thermodynamic limit. Here, the term 'anomaly' means the divergence, that is, usually a phase transition. In Chapter 5, we indicate that our numerical results are consistent with available exact solutions to investigate the behavior of A. In Chapter 6, we consider the suggestion referred to the anomaly of χ and A. Then, we show that the anomaly of A is easier to observe than that of χ from the perspective of size dependence. Finally, we summarize this thesis.

Chapter 2

Quantum spin systems

In this chapter, we review some studies of one-dimensional quantum spin systems, which show the exact solutions of magnetization curves and magnetic susceptibility by Bethe ansatz.

2.1 Magnetic susceptibility for Heisenberg chain

In this section, we review Griffiths's work [9], which shows the behavior of magnetic susceptibility in zero magnetic field at zero magnetization and zero temperature. They focus on $S = 1/2$ antiferromagnetic Heisenberg chain as follows

$$\mathscr{H} = 2J \sum_{j=1}^{N} (\hat{S}_j^x \hat{S}_{j+1}^x + \hat{S}_j^y \hat{S}_{j+1}^y + \hat{S}_j^z \hat{S}_{j+1}^z), \tag{2.1}$$

where J is an exchange interaction, $\hat{S}_j^x, \hat{S}_j^y, \hat{S}_j^z$ are the jth site spin operator in the x, y, z direction, and N is the system size. The boundary condition is periodic:

$$\hat{S}_{N+1} \equiv \hat{S}_1.$$

First, the highest eigenvalue E_F and lowest eigenvalue E_{AF} of the chain (2.1) for $J > 0$ are given by

$$E_F = \frac{1}{2} NJ, \tag{2.2}$$

$$E_{AF} = \left(\frac{1}{2} - \ln 2 \right) NJ. \tag{2.3}$$

The second equation works on $N \to \infty$. These energies are derived by Hulthen [10] and des Cloizeaux and Pearson [11], using Bethe ansatz. To a state with energy

E, normalized energies of E_F, E_{AF} are written as follows

$$\epsilon = \frac{1}{2JN}(E_F - E) = \frac{1}{2NJ}\left(\frac{1}{2}NJ - E\right), \tag{2.4}$$

$$\eta = \frac{1}{2JN}(E - E_{AF}) = \frac{1}{2JN}\left(E - \frac{1}{2}NJ + 2NJ\ln 2\right) = \ln 2 - \epsilon, \tag{2.5}$$

where ϵ, η are the highest and lowest energy normalized. They then consider a state $\Phi(n_1, .., n_r)$ where the spins at $n_1, .., n_r$ are down and all other spins are up. The eigenstate of the chain is given by [1]

$$\Phi = \sum_r a(n_1, .., n_r)\Phi(n_1, .., n_r), \tag{2.6}$$

$$a(n_1, .., n_r) = \sum_{P=1}^{r!} \exp i\left(\sum_{j=1}^{r} k_{P_j} n_j + \sum_{j<l} \phi_{P_j P_l}\right), \tag{2.7}$$

where P is the permutation and k is the wave vector and satisfies

$$Nk_j = 2\pi\lambda_j + \sum_{l\neq j} \phi_{jl}, \quad (j = 1, 2, ..., r) \tag{2.8}$$

$$\cot\frac{1}{2}\phi_{jl} = \frac{1}{2}\left[\cot\left(\frac{1}{2}k_j\right) - \cot\left(\frac{1}{2}k_l\right)\right], \quad (-\pi \leq \phi_{jl} \leq \pi) \tag{2.9}$$

$$\epsilon = N^{-1}\sum_{j=1}^{r}(1 - \cos k_j), \tag{2.10}$$

where λ_j is an integer from 0 to $N-1$. The state of smallest eigenvalues E_{AF}, λ_j satisfies

$$\lambda_1 = \frac{1}{2}N - r + 1, \lambda_2 = \lambda_1 + 2, ..., \lambda_r = \lambda_1 + 2(r-1) = \frac{1}{2}N + r - 1, \tag{2.11}$$

where $0 < \lambda_1 \leq \lambda_2 \leq ... \leq \lambda_r < N$ and $\lambda_{j+1} \geq \lambda_j + 2$. Under the condition of λ_j Eq. (2.11), Eq. (2.8), Eq. (2.9), and Eq. (2.10) are replaced in large N limit by integral equation:

$$k(x) = 2\pi x + \frac{1}{2}\int_{1/2-\rho}^{1/2+\rho} \phi(x, y)dy, \tag{2.12}$$

$$\cot\frac{1}{2}\phi(x, y) = \frac{1}{2}\left[\cot\frac{1}{2}k(x) - \cot\frac{1}{2}k(y)\right], \quad (-\pi \leq \phi \leq \pi) \tag{2.13}$$

$$\epsilon = \frac{1}{2}\int_{1/2-\rho}^{1/2+\rho}[1 - \cos k(x)]dx, \tag{2.14}$$

where $x = \lambda_j/N$, $k(x) = k_j$, and ρ is

$$\frac{1}{2}N - S = N\rho, \tag{2.15}$$

$$\sigma \equiv \frac{S}{N} = \frac{1}{2} - \rho, \tag{2.16}$$

where S is a total spin and σ corresponds to magnetization per site. Then, differentiating both sides of Eq. (2.12) with respect to x, they obtain integral equation:

$$f(\xi) = g_0(\xi) - \int_{-\alpha}^{\alpha} K(\xi - \eta) f(\eta) d\eta, \tag{2.17}$$

where $\xi = \cot(\frac{1}{2}k)$, $f(\xi) = -\frac{dx}{d\xi}$, $g_0(\xi) = \frac{2}{\pi(1+\xi^2)}$, and $K(\xi - \eta) = \frac{2}{\pi(4+(\xi-\eta)^2)}$. On the basis of the integral equation, energies are calculated for antiferromagnetic Heisenberg chain for magnetization $\sigma \to 0$ that corresponds to $\alpha \to \infty$. Subsequently, they consider the σ and η. Solving the integral equation, they obtain

$$\eta = C_1 \left(1 + \frac{1}{2\ln\sigma}\right)\sigma^2 + \mathcal{O}\left(\frac{\sigma^2 \ln|\ln\sigma|}{(\ln\sigma)^2}\right), \tag{2.18}$$

where C_1 is a constant. From integral equations, the relation between the σ and η is revealed.

Next, let us consider the Hamiltonian in the presence of a magnetic field h:

$$\hat{\mathscr{H}}_z = -h \sum_{j=1}^{N} \hat{S}_j^z. \tag{2.19}$$

The lowest energy E_{total} of total Hamiltonian including Eq. (2.1) and Eq. (2.19) is given by

$$E_{total} = E(N, \sigma) - hN\sigma, \tag{2.20}$$

$$E(N, \sigma) = 2NJ\eta(\sigma) + E_{AF}, \tag{2.21}$$

where $E(N, \sigma)$ is the lowest energy of the chain (2.1) and is same as $E(N, M)$ of Eq. (1.3). Differentiating the both sides of Eq. (2.20) with respect to total spin $S = N\sigma$ under $\frac{\partial E_{total}}{\partial S} = 0$, they obtain

$$\frac{1}{N}\frac{\partial E(N,\sigma)}{\partial\sigma} - h = 0$$

$$2\eta'(\sigma) = \frac{h}{J}. \tag{2.22}$$

$\eta'(\sigma)$ is proportional to magnetic field h. The magnetization per spin m is given by differentiating E_{total} with respect to h.

$$m = -\frac{1}{N}\frac{\partial E_{total}}{\partial h} = \sigma. \tag{2.23}$$

Subsequently, the magnetic susceptibility χ is derived:

$$\chi = \frac{\mathrm{d}m}{\mathrm{d}h} = \lim_{h\to 0}\frac{m}{h} = \frac{\sigma}{2J\eta'(\sigma)}.$$

From Eq. (2.18), $\eta'(\sigma)$ is written in the following way

$$\begin{aligned}\eta'(\sigma) &= -\frac{C_1}{2}\frac{\sigma^2}{(\ln\sigma)^2\sigma} + C_1\left(1+\frac{1}{2\ln\sigma}\right)\times 2\sigma \\ &= C_1\sigma\left(2+\frac{\ln\sigma - 1/2}{(\ln\sigma)^2}\right).\end{aligned} \tag{2.24}$$

Thus, χ is represented as

$$\chi = \frac{\sigma}{2J\eta'(\sigma)} = \frac{1}{2JC_1\left(2+\frac{\ln\sigma-1/2}{(\ln\sigma)^2}\right)}. \tag{2.25}$$

The relations between χ, m, and h are shown in Fig. 2.1. Figure 2.1(a) indicates that the magnetization curve is smooth. Conversely, Fig. 2.1(b) shows that χ has a cusp and infinite slope at zero field $h = 0$. This infinite slope is shown by differentiating χ with respect to σ:

$$\begin{aligned}\frac{\partial\chi}{\partial\sigma} &\simeq \frac{1}{4JC_1}\frac{\partial}{\partial\sigma}\left(1-\frac{\ln\sigma-1/2}{(\ln\sigma)^2}\right) \\ &= -\frac{1}{4JC_1}(\ln\sigma)^{-2}\sigma^{-1}\left(1-(\ln\sigma)^{-1}\right).\end{aligned} \tag{2.26}$$

When $\sigma \to 0$ is equal to zero magnetization from Eq. (2.23), the slope of χ becomes infinite from Eq. (2.26) as σ^{-1} diverges quickly compared to $(\ln\sigma)^{-2}$.

2.2 General properties of XXZ chain

In this section, we review Yang and Yang's work [12], which shows the analytic solutions of magnetization curve, magnetic susceptibility, and high-order differential of $S = 1/2$ XXZ chain. First, they introduce $S = 1/2$ XXZ chain Hamiltonian:

$$\hat{\mathscr{H}} = 2J\sum_{j=1}^{N}(\hat{S}^x_j\hat{S}^x_{j+1} + \hat{S}^y_j\hat{S}^y_{j+1} + \Delta\hat{S}^z_j\hat{S}^z_{j+1}), \tag{2.27}$$

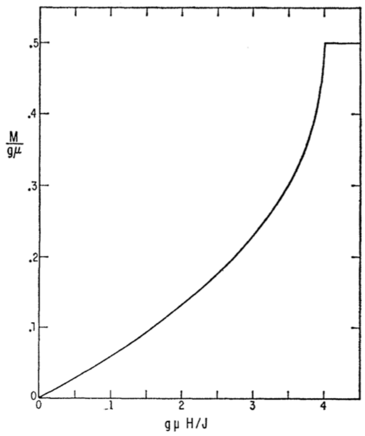

(a) Magnetization as a function of magnetic field at $T = 0$.

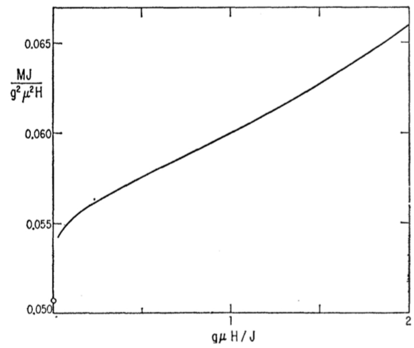

(b) Magnetic susceptibility to a magnetic field at $T = 0$.

Fig. 2.1: Magnetization and magnetic susceptibility reproduced from [9]. Panel (a) demonstrates the curve of a magnetization $m = M/g\mu$ and $h = g\mu H$ where g, μ, and H are the electron g factor, Bohr magneton, and constant. The curve is smooth. Panel (b) demonstrates that $\chi = \lim_{h\to 0} m/h = MJ/g^2\mu^2 H$ has a cusp and infinite slope at zero field $h = 0$.

where $\hat{S}_j^x, \hat{S}_j^y, \hat{S}_j^z$ are the jth site spin operator in the x, y, z direction and N is the system size. For $\Delta = 1$, the system corresponds to the antiferromagnetic chain, while for $\Delta = -1$ it corresponds to the ferromagnetic chain. The Hamiltonian in the presence of a magnetic field h is defined as

$$\hat{\mathscr{H}_z} = -h \sum_{j=1}^{N} \hat{S}_j^z. \tag{2.28}$$

The lowest energy E_{total} of total Hamiltonian adding Eq. (2.28) to Eq. (2.27) is given by

$$E_{total} = N(2\epsilon(m) - hm), \tag{2.29}$$

where $\epsilon(m)$ is the lowest energy per site of Hamiltonian (2.27) and m is the magnetization. The magnetic field h and magnetic susceptibility χ is defined as [13]

$$h = 2\frac{\partial \epsilon(m)}{\partial m}, \tag{2.30}$$

$$\chi = \left(2\frac{\partial^2 \epsilon(m)}{\partial m^2}\right)^{-1}. \tag{2.31}$$

Through these quantity, they consider the magnetization curve of the system for various values of Δ. First, for $\Delta = 0$, the lowest energy of the Hamiltonian is written in the form [13]

$$\epsilon(m) = -\frac{1}{\pi}\cos\frac{\pi m}{2}. \tag{2.32}$$

Substituting Eq. (2.30) and Eq. (2.31) for Eq. (2.32), they obtain

$$h = \sin\frac{\pi m}{2}, \tag{2.33}$$

$$\chi^{-1} = \frac{\pi}{2}\cos\frac{\pi m}{2}. \tag{2.34}$$

For zero magnetization, $h(m=0) = 0$ and $\chi^{-1}(m=0) = \pi/2$.

Next, for $-1 < \Delta < 1$, the lowest energy of the Hamiltonian is given by [13]

$$\epsilon(m) - \epsilon(0) = \frac{\pi(\pi-\mu)\sin\mu}{8\mu}m^2(1 + \mathcal{O}(m^2) + \mathcal{O}(m^{\frac{4\mu}{\pi-\mu}})), \tag{2.35}$$

where $\mu = \arccos(\Delta)$. From Eq. (2.35), h and χ^{-1} are derived:

$$h = \frac{\pi(\pi-\mu)\sin\mu}{4\mu}(2m + \mathcal{O}(m^3) + \mathcal{O}(m^{\frac{4\mu}{\pi-\mu}+1})), \tag{2.36}$$

$$\chi^{-1} = \frac{\pi(\pi-\mu)\sin\mu}{4\mu}(2 + \mathcal{O}(m^2) + \mathcal{O}(m^{\frac{4\mu}{\pi-\mu}})). \tag{2.37}$$

At zero magnetization, $h(m=0) = 0$ and $\chi^{-1}(m=0) = \frac{\pi(\pi-\mu)\sin\mu}{2\mu}$. In addition, they derive the nth derivative of the energy as follows

$$\lim_{m\to 0+}\left(\frac{d}{dm}\right)^n \epsilon(m) = \begin{cases} \text{finite} & \left(n < 2 + \frac{4\mu}{\pi-\mu}\right) \\ \pm\infty & \left(n > 2 + \frac{4\mu}{\pi-\mu}\right) \end{cases}, \tag{2.38}$$

where $\frac{4\mu}{\pi-\mu}$ is irrational. Subsequently, introducing $\chi^{-1} = 2\frac{d^2\epsilon(m)}{dm^2}$, they obtain

$$\lim_{m\to 0+}\left(\frac{d}{dm}\right)^n \chi^{-1} = \begin{cases} \text{finite} & \left(n < \frac{4\mu}{\pi-\mu}\right) \\ \pm\infty & \left(n > \frac{4\mu}{\pi-\mu}\right) \end{cases}. \tag{2.39}$$

However, when $\frac{4\mu}{\pi-\mu}$ is an integer, individual discussion is needed. The correspondence between $\frac{4\mu}{\pi-\mu}$ which is an integer and Δ is

$$\frac{4\mu}{\pi-\mu} = 4 \leftrightarrow \Delta = 0,$$
$$\frac{4\mu}{\pi-\mu} = 3 \leftrightarrow \Delta \simeq 0.22,$$
$$\frac{4\mu}{\pi-\mu} = 2 \leftrightarrow \Delta = 1/2,$$
$$\frac{4\mu}{\pi-\mu} = 1 \leftrightarrow \Delta = \frac{1+\sqrt{5}}{4} \simeq 0.81.$$

The lowest energy for $\Delta = 0$ is Eq. (2.32). Other cases are not discussed.

Finally, for $\Delta < -1$, the lowest energy is written in the form [13]

$$\epsilon(m) - \epsilon(0) = \frac{\sinh\lambda}{2\pi}\left(2\pi e_0 m + \frac{2\pi^3}{3}\frac{e_2}{e_0^2}m^3 + \mathcal{O}(m^4)\right), \tag{2.40}$$
$$\sum_{n=-\infty}^{\infty}\frac{(-1)^n\cos n\sigma}{2\cosh n\lambda} = e_0 + e_2\sigma^2 + e_4\sigma^4 + ...,$$

where $\Delta = \cosh\lambda$ and e_0, e_2, e_4 are constants. From Eq. (2.40), h and χ^{-1} are represented as

$$\begin{aligned}
h &= \frac{\sinh\lambda}{\pi}\left(2\pi e_0 + 2\pi^3\frac{e_2}{e_0^2}m^2 + \mathcal{O}(m^3)\right) \\
&= 2\sinh\lambda\left(e_0 + e_2\left(\frac{\pi m}{e_0}\right)^2 + \mathcal{O}(m^3)\right) \\
&= 2\sinh\lambda\sum_{n=-\infty}^{\infty}\frac{(-1)^n\cos n\frac{\pi m}{e_0}}{2\cosh n\lambda}, \\
\chi^{-1} &= \frac{\sinh\lambda}{\pi}\left(4\pi^3\frac{e_2}{e_0^2}m + \mathcal{O}(m^2)\right).
\end{aligned}$$

For zero magnetization, h and χ^{-1} are written in the form

$$\begin{aligned}
h(m=0) &= 2\sinh\lambda\sum_{n=-\infty}^{\infty}\frac{(-1)^n}{2\cosh n\lambda} \\
&= \frac{\pi\sinh\lambda}{\lambda}\sum_{n=-\infty}^{\infty}\text{sech}\frac{\pi^2}{2\lambda}(1+2n), \qquad (2.41)\\
\chi^{-1}(m=0) &= 0. \qquad (2.42)
\end{aligned}$$

These behaviors of h and χ^{-1} are shown in Fig. 2.2. Figure 2.2 shows that $h(m = 0) = 0$ for $-1 < \Delta < 1$ and $h(m = 0) =$ finite for $|\Delta| > 1$. This indicates that the system is gapless for $-1 < \Delta < 1$ and is gapped for $|\Delta| > 1$, as the magnetic field $h(m = 0)$ means the energy gap of the system from Eq. (2.30).

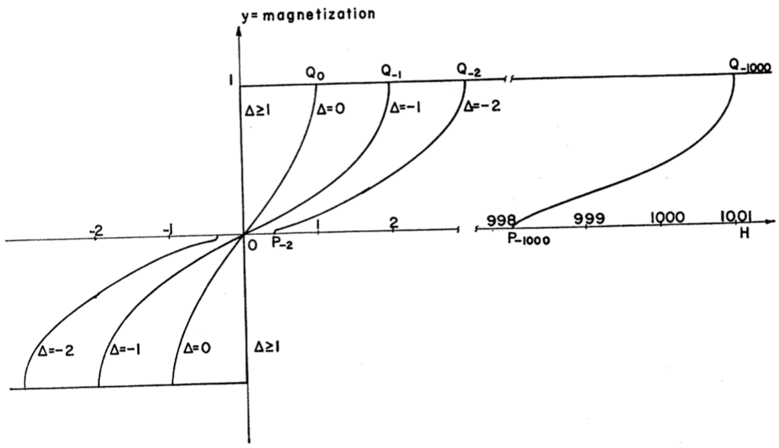

Fig. 2.2: Magnetization $m = y$ at a magnetic field $h = H$ for anisotropic parameter $\Delta \to -\Delta$ reproduced from [12]. The system is gapless for $-1 < \Delta < 1$ and is gapped for $|\Delta| > 1$, as the magnetic field $h(m = 0)$ means the energy gap of the system.

2.3 Behavior of ground state energy

In this section, we review Lukyanov's work [14], which shows the detail behavior of ground state energy for $S = 1/2$ XXZ chain for $-1 < \Delta < 1$ that is anisotropic parameter, comparing with Eq. (2.35). They focus on the chain:

$$\hat{\mathscr{H}} = 2J \sum_{j=1}^{N} \left[\hat{S}_j^x \hat{S}_{j+1}^x + \hat{S}_j^y \hat{S}_{j+1}^y + \Delta \left(\hat{S}_j^z \hat{S}_{j+1}^z - \frac{1}{2} \right) \right], \tag{2.43}$$

where J is an exchange interaction and positive, $\hat{S}_j^x, \hat{S}_j^y, \hat{S}_j^z$ are the jth site spin operator in the x, y, z direction, and N is the system size and even. The boundary condition is defined as

$$\hat{S}_1^{\pm} = e^{\pm 2\pi i \theta} \hat{S}_{N+1}^{\pm}, \tag{2.44}$$

$$\hat{S}_1^z = \hat{S}_{N+1}^z, \tag{2.45}$$

where $\hat{S}_j^{\pm} = \hat{S}_j^x \pm i\hat{S}_j^y$ and θ is real parameter that takes the value from 0 to 1, that is, $0 < \theta < 1$. In addition, the unitary transformation to spin operator is given in the form

$$\hat{U}^+\hat{S}_j^x\hat{U} = (-1)^j\hat{S}_j^x, \quad \hat{U}^+\hat{S}_j^y\hat{U} = (-1)^j\hat{S}_j^y, \quad \hat{U}^+\hat{S}_j^z\hat{U} = \hat{S}_j^z, \tag{2.46}$$

where $\hat{U} = \exp\left(i\pi\sum_k k\hat{S}_k^z\right)$ is a unitary matrix. Acting on Hamiltonian (2.43), they obtain

$$\begin{aligned}\hat{U}^+\mathscr{H}\hat{U} &= 2J\sum_{k=1}^{N}(-\hat{S}_j^x\hat{S}_{j+1}^x - \hat{S}_j^y\hat{S}_{j+1}^y + \Delta(\hat{S}_j^z\hat{S}_{j+1}^z - 1)) \\ &= -2J\sum_{k=1}^{N}(\hat{S}_j^x\hat{S}_{j+1}^x + \hat{S}_j^y\hat{S}_{j+1}^y - \Delta(\hat{S}_j^z\hat{S}_{j+1}^z - 1)).\end{aligned} \tag{2.47}$$

Comparing Eq. (2.47) with Eq. (2.43), both equations are equivalent when $J \leftrightarrow -J, \Delta \leftrightarrow -\Delta$. Thus, the system for $J > 0$ is equal to the system for $J < 0$. For convenience, Δ and J are parameterized as follows

$$\Delta = \cos(\pi\beta^2), \tag{2.48}$$

$$J = \frac{1-\beta^2}{\sin(\pi\beta^2)}a^{-1}, \tag{2.49}$$

where $a > 0$ and $0 < \beta^2 \leq 1$. Subsequently, they define the ground state energy of the chain in a magnetic field h as

$$\epsilon(h) = \lim_{N\to\infty}\frac{E_{total}(h)}{N}, \tag{2.50}$$

where $\epsilon(h)$ is the ground state energy $E_{total}(h)$ per site. The ground state energy per site $\epsilon(h)$ is explicitly given by [13]

$$\epsilon(h) = -\frac{h}{4} + J\int_{-\Lambda}^{\Lambda}\frac{d\alpha}{2\pi}\frac{\sin(\pi\beta^2)\,f(\alpha)}{\cosh(2\alpha)+\cos(\pi\beta^2)}, \tag{2.51}$$

$$f(\alpha) - \int_{-\Lambda}^{\Lambda}\frac{d\alpha'}{\pi}\frac{\sin(2\pi\beta^2)\,f(\alpha')}{\cosh(2\alpha-2\alpha')-\cos(2\pi\beta^2)} = \frac{h}{J} - \frac{4\sin^2(\pi\beta^2)}{\cosh(\alpha)+\cos(2\pi\beta^2)},$$
$$f(\pm\Lambda) = 0.$$

Using Wiener-Hopf method that solves integral equations by decomposing an arbitrary function Φ into $\Phi_+ = \frac{1}{2\pi i}\int_{C_1}\Phi(z)\frac{z}{z-\alpha}$ and $\Phi_- = \frac{1}{2\pi i}\int_{C_2}\Phi(z)\frac{z}{z-\alpha}$ where

C_1 and C_2 are parallel contours to real line, the ground state energy $\epsilon(h)$ is derived:

$$\epsilon(h) = \mathcal{E}_0 - \frac{ah^2}{16\pi\beta^2}\left(1 + \kappa|ah|^{\frac{4}{\beta^2}-4} + (\kappa_+ + \kappa_-)(ah)^2 + \dots\right), \tag{2.52}$$

$$\mathcal{E}_0 = -\frac{2}{\pi a}\left(1-\beta^2\right)\int_0^\infty dt \frac{\sinh\left(\beta^2 t\right)}{\sinh(t)\cosh\left(\left(1-\beta^2\right)t\right)}. \tag{2.53}$$

where

$$\kappa = \frac{\Gamma^2\left(\beta^{-2}\right)\tan\left(\pi\beta^{-2}\right)}{2\beta^2\Gamma^2\left(\frac{1}{2}+\beta^{-2}\right)}\left[\frac{\Gamma\left(\frac{\beta^2}{2-2\beta^2}\right)}{8\sqrt{\pi}\Gamma\left(\frac{1}{2-2\beta^2}\right)}\right]^{\frac{2}{\beta^2}-2}, \tag{2.54}$$

$$\kappa_+ = \frac{1}{64\pi\beta^2}\tan\left(\frac{\pi}{2-2\beta^2}\right), \tag{2.55}$$

$$\kappa_- = \frac{1}{192\pi}\frac{\Gamma\left(\frac{3}{2-2\beta^2}\right)\Gamma^3\left(\frac{\beta^2}{2-2\beta^2}\right)}{\Gamma\left(\frac{3\beta^2}{2-2\beta^2}\right)\Gamma^3\left(\frac{1}{2-2\beta^2}\right)}. \tag{2.56}$$

Here, the magnetic field h is assumed to be small ($|h/J| \ll 1$). In addition, carrying out the exchange of h and a magnetization m from Legendre transformation, the magnetic susceptibility $\chi = \frac{\partial^2\epsilon(m)}{\partial m^2}$ is described as follows

$$\chi \simeq -\frac{a}{8\pi\beta^2}\left[1 - \frac{\kappa}{2}\left(\frac{4}{\beta^2}-2\right)\left(\frac{4}{\beta^2}-3\right)|am|^{\frac{4}{\beta^2}-4} - 6a(\kappa_+ + \kappa_-)m^2 + ...\right]. \tag{2.57}$$

These indicate that the ground state energy and magnetic susceptibility in the presence of a magnetic field are derived in detail, compared with Eq. (2.35) and Eq. (2.37).

Chapter 3

Theory

In this chapter, we introduce the physical procedure of calculating the magnetic susceptibility χ and fourth derivative A of energy as a function of magnetization. In addition, we introduce the free boson model and sine-Gordon model describing the critical phenomena and low-energy behavior of the $S = 1/2$ XXZ antiferromagnetic chain treated in our study. We formulate the behavior of magnetic susceptibility χ and fourth derivative A.

3.1 Energy and correction term

The total spin operator in the z direction $\hat{S}_T^z$ is defined as

$$\hat{S}_T^z \equiv \sum_{j=1}^{N} \hat{S}_j^z, \tag{3.1}$$

where $\hat{S}_j^z$ is the jth site spin operator in the z direction and N is the system size. This operator and a Hamiltonian $\hat{\mathscr{H}}$ that shows $U(1)$ symmetry commute: $[\hat{\mathscr{H}}, \hat{S}_T^z] = 0$. From the commutation relation, we obtain

$$\hat{\mathscr{H}} \left|\psi\right\rangle = E(N, M) \left|\psi\right\rangle, \tag{3.2}$$

$$\hat{S}_T^z \left|\psi\right\rangle = M \left|\psi\right\rangle, \ (M = 0, \pm 1, ..., \pm N/2) \tag{3.3}$$

where $E(N, M)$ is the lowest energy, M is the magnetization, and $|\phi\rangle$ is the eigenstate. We note that $|\phi\rangle$ is a simultaneous eigenstate of $\hat{\mathscr{H}}$ and $\hat{S}_T^z$. For $N \to \infty$, the energy of $\hat{\mathscr{H}}$ per site, $\epsilon(m)$, is then given by [15]

$$\lim_{N\to\infty} \frac{E(N, M)}{N} = \epsilon(m), \tag{3.4}$$

where $m = M/N$ is the magnetization per site. When N is finite, Eq. (3.4) is written as following

$$\frac{E(N,M)}{N} = \epsilon(m) + C(N,m), \tag{3.5}$$

where $C(N,m)$ is a correction term of a finite size. Generally, $\epsilon(m)$ is analytic for m in the thermodynamic limit. The term 'analytic' indicates that a function and high-order differential are continuous. However, in this thesis, high-order differential is defined as derivative up to fourth derivative. Then, the correction term $C(N,m)$ satisfies the following conditions:

$$\lim_{N\to\infty} C(N,m) = 0, \tag{3.6}$$

$$\lim_{N\to\infty} C^{(n)}(N,m) = 0,\ (n \geq 1) \tag{3.7}$$

where $C^{(n)}(N,m)$ is the nth derivative of the correction term with respect to magnetization. The correction term depends on the boundary conditions and dimension. The details are discussed in Section 6.3.

3.2 Magnetic susceptibility and fourth derivative

Using energy per site $\epsilon(m)$, high-order differentials such as the magnetic susceptibility χ and fourth derivative A are defined in the following way

$$\chi \equiv \frac{1}{\epsilon''(m)}, \tag{3.8}$$

$$A \equiv \frac{\partial^2}{\partial m^2}\chi^{-1} = \frac{\partial^4}{\partial m^4}\epsilon(m). \tag{3.9}$$

The difference between the lowest energies $E(N, M)$ is explicitly described by χ and A as follows

$$
\begin{aligned}
&\epsilon''(N, m) \\
&\equiv N\{E(N, M+1) - 2E(N, M) + E(N, M-1)\} \\
&= \chi^{-1} + C''(N, m) + \frac{1}{12N^2}\left(\epsilon^{(4)}(m) + C^{(4)}(N, m)\right) \\
&+ \mathcal{O}\left(\frac{1}{N^4}\right),
\end{aligned}
\tag{3.10}
$$

$$
\begin{aligned}
&\epsilon^{(4)}(N, m) \\
&\equiv N^3\{E(N, M+2) - 4E(N, M+1) + 6E(N, M) \\
&- 4E(N, M-1) + E(N, M-2)\} \\
&= A + C^{(4)}(N, m) + \frac{1}{6N^2}\left(\epsilon^{(6)}(m) + C^{(6)}(N, m)\right) \\
&+ \mathcal{O}\left(\frac{1}{N^4}\right),
\end{aligned}
\tag{3.11}
$$

where $\epsilon^{(n)}(N, m)$ is the nth finite-difference between the lowest energies. $\epsilon(N, m)$ is obtained directly from our numerical results in finite systems. We then consider the behavior of $\epsilon''(N, m)$ and $\epsilon^{(4)}(N, m)$. As an example, we consider the $S = 1/2$ XXZ antiferromagnetic chain that has $U(1)$ symmetry and an anisotropic parameter Δ in the z component. When $\Delta \gg 1$ and there is a Neel state which indicates an energy gap, the lowest energy $E(N, M)$ is described as

$$
E(N, M) = E(N, 0) + |M|\Delta E, \tag{3.12}
$$

where ΔE is an energy gap for a finite system. Using Eq. (3.12), in the thermodynamic limit, Eq. (3.10) can be rewritten as

$$
\epsilon''(N, m) = \begin{cases} N(2\Delta E) & (m = 0), \\ 0 & (m \neq 0). \end{cases} \tag{3.13}
$$

Similarly, substituting Eq. (3.12) into Eq. (3.11), we obtain

$$
\epsilon^{(4)}(N, m) = \begin{cases} N^3(-4\Delta E) & (m = 0), \\ N^3(2\Delta E) & (m = \pm 1/N), \\ 0 & (m \neq 0, \pm 1/N). \end{cases} \tag{3.14}
$$

However, for a case of finite anisotropy, $\epsilon''(N, m)$ and $\epsilon^{(4)}(N, m)$ become nonzero at $m \neq 0, 1/N$ region because of interactions between magnons. Thus, for large

N, we give $\epsilon''(N,m)$ and $\epsilon^{(4)}(N,m)$ as follows

$$\epsilon''(N,m) = \begin{cases} N(2\Delta E) & (m=0), \\ \text{finite} & (m \neq 0), \end{cases} \tag{3.15}$$

$$\epsilon^{(4)}(N,m) = \begin{cases} N^3(-4\Delta E) & (m=0), \\ N^3(2\Delta E) & (m=\pm 1/N), \\ \text{finite} & (m \neq 0, \pm 1/N). \end{cases} \tag{3.16}$$

These relations mean that $\epsilon^{(4)}(N,m)$ is N^2 times as large as $\epsilon''(N,m)$. The anomaly of A appears stronger than that of χ^{-1} in the thermodynamic limit. In addition, from Eq. (3.16), the behavior of $\epsilon^{(4)}(N,m)$ at $m=0$ and $m=1/N$ is different. Thus, we introduce A as physical concept for observing an anomaly.

Next, we discuss the case in which $\epsilon(m)$ is not analytic. $\epsilon(m)$ is not analytic for m when $\epsilon''(N,m)$ or $\epsilon^{(4)}(N,m)$ diverges. In the thermodynamic limit, the relation is given by

$$\begin{cases} \lim_{N\to\infty} \epsilon''(N,m) = \epsilon''(m) & (3.17) \\ \qquad \Rightarrow \epsilon(m) \text{ is analytic,} \\ \lim_{N\to\infty} \epsilon''(N,m) = \pm\infty & (3.18) \\ \qquad \Rightarrow \epsilon(m) \text{ is not analytic.} \end{cases}$$

The same holds for $\epsilon^{(4)}(N,m)$. The divergence of $\epsilon''(N,m)$ and $\epsilon^{(4)}(N,m)$ is equivalent to the fact that χ^{-1} and A diverge.

3.3 Free boson

We introduce the free boson which indicates the critical phenomena of the $S=1/2$ XXZ antiferromagnetic chain. The basics of conformal field theory is introduced in Appendix D. First, for simplicity, we consider a free boson field $X(z,\overline{z})$ and an action S.

$$\begin{aligned} S &= \frac{1}{4\pi\alpha'}\int d^2x(\nabla X)^2 = \frac{1}{4\pi\alpha'}\int d^2x\left(\left(\frac{\partial X}{\partial x_1}\right)^2 + \left(\frac{\partial X}{\partial x_2}\right)^2\right) \\ &= \frac{1}{4\pi\alpha'}\int d^2x[(\partial z X + \partial\overline{z}X)^2 - (\partial z X - \partial\overline{z}X)^2] \\ &= \frac{1}{\pi\alpha'}\int d^2z \partial z X \partial\overline{z}X, \end{aligned} \tag{3.19}$$

where α' is parameter which has length L^2 dimension, $z = x_1 + ix_2, \overline{z} = x_1 - ix_2$, $\partial z \equiv \frac{1}{2}(\partial x_1 - i\partial x_2), \partial\overline{z} \equiv \frac{1}{2}(\partial x_1 + i\partial x_2)$, and $d^2x = \frac{d\overline{z}\wedge dz}{2i} \equiv d^2z$. From an Euler-Lagrange equation, we obtain

$$\partial z\partial\overline{z}X = 0. \tag{3.20}$$

From Eq. (3.20), $X(z,\overline{z})$ is a function of z or $\overline{z}$. Therefore, the free boson field $X(z,\overline{z})$ is divided into holomorphic part and antiholomorphic part.

$$X(z,\overline{z}) = X(z) + \overline{X}(\overline{z}), \tag{3.21}$$

where $X(z)$ is a left-mover and $\overline{X}(\overline{z})$ is a right-mover.

Next, we consider a two-point correlation function. The two-point correlation function of the physical quantity x, x' is given:

$$\langle x_q x_r\rangle = A^{-1}_{qr} \equiv G_{rq} \to \int dx A(x,x')G(x') = \delta(x-x'), \tag{3.22}$$

where G_{rq} and $G(x')$ are Green function and A_{qr} and $A(x,x')$ is the term involved in a gauss integral:

$$\int d\boldsymbol{x} \exp\left[-\frac{1}{2}{}^t\boldsymbol{x}A\boldsymbol{x}\right] = (2\pi)^{\frac{N}{2}}(\det A)^{-\frac{1}{2}}, \tag{3.23}$$

where A is matrix and $\boldsymbol{x}$ is vector. The term corresponding to A_{qr} in the action S is $\partial z\partial\overline{z}$. Thus, the correlation function of the fields is derived from

$$\begin{aligned}\langle X(z,\overline{z})X(\omega,\overline{\omega})\rangle &= \frac{1}{Z}\int X(z,\overline{z})X(\omega,\overline{\omega})e^{-S(X)} \\ &= \frac{1}{2}\left(-\frac{1}{\pi\alpha'}\partial z\partial\overline{z}\right)^{-1}\delta(z-\omega,\overline{z}-\overline{\omega}) \\ \partial z\partial\overline{z}\langle X(z,\overline{z})X(\omega,\overline{\omega})\rangle &= -\frac{\pi\alpha'}{2}\delta(z-\omega,\overline{z}-\overline{\omega}),\end{aligned} \tag{3.24}$$

where Z is a partition function. The formula of Green function in two dimension is written in the form

$$\Delta \ln|z| = 4\partial z\partial\overline{z}\ln|z| = 2\pi\delta^2(z,\overline{z}), \tag{3.25}$$

where $\delta^2(z,\overline{z}) = \delta(z)\delta(\overline{z})$. Comparing Eq. (3.24) with Eq. (3.25), we obtain

$$\begin{aligned}\partial z\partial\overline{z}\langle X(z,\overline{z})X(\omega,\overline{\omega})\rangle &= -\frac{\pi\alpha'}{2}\delta(z-\omega,\overline{z}-\overline{\omega}) \\ &= -\frac{\alpha'}{2}\partial z\partial\overline{z}\ln|z-\omega|^2.\end{aligned}$$

Thus, the two-point correlation function of $X(z, \overline{z})$ and $X(\omega, \overline{\omega})$ is

$$\begin{aligned}\langle X(z, \overline{z}) X(\omega, \overline{\omega})\rangle &= -\frac{\alpha'}{2} \ln |z-\omega|^2 \\ &= -\frac{\alpha'}{2} \ln (z-\omega) - \frac{\alpha'}{2} \ln (\overline{z}-\overline{\omega}).\end{aligned} \tag{3.26}$$

From Eq. (3.21), the two-point correlation function of $X(z)$ and $X(\overline{z})$ is

$$\langle X(z) X(\omega)\rangle = -\frac{\alpha'}{2} \ln (z-\omega), \langle \overline{X}(\overline{z}) \overline{X}(\overline{\omega})\rangle = -\frac{\alpha'}{2} \ln (\overline{z}-\overline{\omega}). \tag{3.27}$$

Subsequently, it is convenient to define the current $J(z)$ as

$$J(z) \equiv \left(\frac{2}{\alpha'}\right)^{1/2} i\partial z X(z). \tag{3.28}$$

The product of $J(z)$ is written in the form

$$J(z) J(\omega) = -\left(\frac{2}{\alpha'}\right) \partial z \partial \omega X(z) X(\omega) \simeq \frac{1}{(z-\omega)^2}. \tag{3.29}$$

Using $J(z)$, a stress-energy tensor $T(z)$ which means Noether's current is

$$T(z) = \frac{1}{2} : J(z) J(z) :\equiv \frac{1}{2} \lim_{\omega \to z} \left[J(\omega) J(z) - \frac{1}{(z-\omega)^2}\right]. \tag{3.30}$$

The sign ': :' is a normal order product where the annihilation operator is aligned to the right of the generation operator. For convenience, the current J is expanded for a Laurent expansion.

$$J(z) = \left(\frac{2}{\alpha'}\right)^{1/2} i\partial z X(z) = \alpha_0 z^{-1} + \sum_{n \neq 0} \alpha_n z^{-n-1} = \sum_{n \in \mathbb{Z}} \alpha_n z^{-n-1}. \tag{3.31}$$

Similarly, the field $X(z)$ is derived:

$$X(z) = \left(\frac{\alpha'}{2}\right)^{1/2} \left[\phi_0 - i\alpha_0 \ln z + i \sum_{n \neq 0} \frac{\alpha_n}{n} z^{-n}\right], \tag{3.32}$$

where ϕ_0 is a zero mode. We then derive a commutation relation of the expansion coefficient α_n. Using $\alpha_n = \oint \frac{dz}{2\pi i} z^n J(z)$, we obtain the following relation

$$\begin{aligned}[\alpha_m, \alpha_n] &= \left[\oint \frac{dz}{2\pi i} z^m J(z), \oint \frac{d\omega}{2\pi i} \omega^n J(\omega)\right] \\ &= i^2 \oint_{|z|>|\omega|} \frac{dz}{2\pi i} z^m \partial z X(z) \oint_{\omega=0} \frac{d\omega}{2\pi i} \omega^n \partial \omega X(\omega) \\ &- i^2 \oint_{|z|<|\omega|} \frac{d\omega}{2\pi i} \omega^n \partial \omega X(\omega) \oint_{z=0} \frac{dz}{2\pi i} z^m \partial z X(z) \\ &= m\delta_{m+n,0},\end{aligned} \tag{3.33}$$

where $\oint_{|z|>|\omega|}$ is path integral for the region of $|z| > |\omega|$, $\oint_{\omega=0}$ is integral path around $\omega = 0$, $\oint_{|z|<|\omega|}$ is path integral for the region $|z| < |\omega|$, $\oint_{z=0}$ is integral path around $z = 0$. Furthermore, the product of $J(z)$ and $X(z)$ is derived from Eq. (3.27).

$$J(z)X(\omega) = i\left(\frac{2}{\alpha'}\right)^{1/2} \partial z X(z)X(\omega) \simeq -i\left(\frac{\alpha'}{2}\right)^{1/2} \frac{1}{z-\omega}.$$

Using the above equation, the commutation relation between α_n and $\phi_0 = \oint \frac{dz}{2\pi i}X(z)$ is given by

$$\begin{aligned}[\alpha_m, \phi_0] &= \left[\oint \frac{dz}{2\pi i} z^m J(z), \oint \frac{d\omega}{2\pi i} X(\omega)\right] \\ &= \oint_{\omega=0} \frac{d\omega}{2\pi i} \oint_{z=\omega} \frac{dz}{2\pi i} z^m J(z)X(\omega) \\ &= -i\delta_{m,0}. \end{aligned} \tag{3.34}$$

The α_n for $n > 0$ is regarded as annihilation operator and that for $n < 0$ is regarded as a creation operator. In other words, α_n and α_{-n} are Hermitian conjugate. When $\alpha_n = \sqrt{n}a_n, \alpha_{-n} = \sqrt{n}a_n^\dagger$, $a_n, a_n^\dagger$ are a creation and an annihilation operator. Similarly, the creation and annihilation operator and zero mode are defined as $\tilde{\alpha}_n$ and $\overline{\phi}_0$ in an antiholomorphic part.

Finally, we introduce a vertex operator as a primary field which plays an important role in a free boson field. The vertex operator with an electric charge (momentum) p is defined in the form

$$\begin{aligned} V_p(z) &\equiv: \exp\left[\left(\frac{2}{\alpha'}\right)^{1/2} ipX(z)\right]: \\ &\equiv \exp\left[p\sum_{n=1}^{\infty} \frac{\alpha_{-n}}{n} z^n\right] \exp\left[-p\sum_{n=1}^{\infty} \frac{\alpha_n}{n} z^{-n}\right] e^{ip\phi_0} z^{p\alpha_0}, \end{aligned} \tag{3.35}$$

where $V_p(z)$ is the primary field with the electric charge p to the current J and the conformal weight $\frac{p^2}{2}$. The Fock state $|p_L, p_R\rangle$ of the vertex operator is defined as

$$|p_L, p_R\rangle = \lim_{z,\bar{z}\to 0} V_{p_L}(z)\overline{V_{p_R}(z)}\,|0\rangle\,, \tag{3.36}$$

$$\alpha_n\,|p_L, p_R\rangle = \tilde{\alpha}_n\,|p_L, p_R\rangle = 0, \quad (n \geq 1) \tag{3.37}$$

$$\alpha_0\,|p_L, p_R\rangle = p_L\,|p_L, p_R\rangle\,, \tag{3.38}$$

$$\tilde{\alpha}_0\,|p_L, p_R\rangle = p_R\,|p_L, p_R\rangle\,, \tag{3.39}$$

where p_L, p_R are an electric charge of the current J, $\tilde{J}$ defined as

$$\alpha_0 \equiv \int \frac{dz}{2\pi i} J(z),$$
$$\tilde{\alpha}_0 \equiv -\int \frac{d\bar{z}}{2\pi i} \tilde{J}(\bar{z}).$$

The products of $J(z)$ and $V_p(\omega)$ and that of $V_p(z)$ and $V_p(\omega)$ are

$$J(z)V_p(\omega) \simeq \frac{p}{z-\omega} V_p(\omega), \tag{3.40}$$
$$T(z)V_p(\omega) \simeq \frac{p^2/2}{(z-\omega)^2} V_p(\omega) + \frac{1}{z-\omega} \partial\omega V_p(\omega). \tag{3.41}$$

From Wick's theorem and Eq. (3.27), we obtain

$$V_{p_1}(z)V_{p_2}(\omega) = (z-\omega)^{p_1 p_2} V_{p_1+p_2}(\omega). \tag{3.42}$$

When $p_1 + p_2 = 0$, the two-point correlation function of the vertex operator is written as

$$V_p(z)V_{-p}(\omega) = \frac{1}{(z-\omega)^{p^2}} V_0(\omega)$$
$$\langle 0| V_p(z)V_{-p}(\omega) |0\rangle = \frac{1}{(z-\omega)^{p^2}}. \tag{3.43}$$

When $p_1 + p_2 \neq 0$, this equation is transformed as

$$\langle 0| V_{p_1}(z)V_{p_2}(\omega) |0\rangle = (z-\omega)^{p_1 p_2} \langle 0| V_{p_1+p_2} |0\rangle = 0. \tag{3.44}$$

The above equation means the conservation of the electric charge.

3.4 Sine-Gordon model

We introduce the sine-Gordon model describing the low-energy behavior of the $S = 1/2$ XXZ antiferromagnetic chain. The sine-Gordon model is an extension of the gaussian (free boson) model. The Lagrangian $\mathcal{L}$ of the sine-Gordon model is defined as

$$\mathcal{L} = \frac{1}{2\pi K}(\nabla\phi)^2 + \frac{y_\phi}{2\pi\alpha^2} \cos\sqrt{8}\phi. \tag{3.45}$$

where K is a parameter and the term $\cos\sqrt{8}\phi$ in Eq. (3.45) means an irrelevant field. Considering the renormalization which shows the behavior of a critical phenomena, when the irrelevant field is ignored, the critical phenomena of the sine-Gordon model is equal to the gaussian model. When the sine-Gordon model is corresponded to XXZ chain which has the antiisotropic parameter Δ of z component, scaling dimension $x_{\alpha,\beta}$ which indicates the critical exponent is written as [16, 17]

$$x_{\alpha,\beta} = \frac{1}{2}\left(\alpha^2 K + \frac{\beta^2}{K}\right) = \frac{1}{2}\left(\alpha^2 \frac{\pi}{\arccos(-\Delta)} + \beta^2 \frac{\arccos(-\Delta)}{\pi}\right), \tag{3.46}$$

$$K = \frac{\pi}{\arccos(-\Delta)}, \tag{3.47}$$

where α, β are integer. The detail properties of gaussian model and sine-Gordon model are discussed in Appendix B. In addition, the way to derive the sine-Gordon model from XXZ chain is discussed in Appendix B.3.

3.5 Behavior of magnetic susceptibility and fourth derivative

Using the conformal field theory describing the low-energy behavior of the $S = 1/2$ XXZ antiferromagnetic chain, we show the behavior of magnetic susceptibility χ and fourth derivative A. The energy gap ΔE for a finite system size N is written as follows

$$\Delta E = E(N, M) - E(N, 0) = \frac{2\pi v}{N} x, \tag{3.48}$$

where v is the velocity of the spin wave which is $v = dE(k)/dk$ for wavenumber k and x is a scaling dimension of primary field, which describes critical phenomena of the system. We extend Eq. (3.48) to the gaussian model case [18]:

$$\Delta E = \frac{2\pi v}{N} x_{0,M} = \frac{2\pi v}{N} \frac{M^2}{2K}$$

$$\frac{\Delta E}{N} = \frac{2\pi v}{N} N \frac{m^2}{2K}, \tag{3.49}$$

$$x_{\alpha,\beta} = \frac{1}{2}\left(\alpha^2 K + \frac{\beta^2}{K}\right), \tag{3.50}$$

where $m = M/N$, $x_{\alpha,\beta}$ is scaling dimension, K is a parameter, and α, β are integer. Subsequently, adding Eq. (3.48) to the irrelevant perturbation, the energy gap ΔE for a finite system size N is given by [19]

$$\Delta E = \frac{2\pi v}{N}\left\{x + C_1\left(\frac{1}{N}\right)^{x_T - 2} + C_2\left(\frac{1}{N}\right)^{2(x_T - 2)}\right\}, \tag{3.51}$$

where x_T is a scaling dimension to irrelevant perturbation that is different from x and C_1, C_2 are constants. We extend Eq. (3.51) to the sine-Gordon model case that corresponds to the $S = 1/2$ XXZ chain:

$$\Delta E = 2\pi v \left|\frac{M}{N}\right|^2 N \left(\frac{1}{2K} + C_1 |m|^{x_T-2} + C_2 |m|^{2(x_T-2)}\right)$$
$$\frac{\Delta E}{N} = 2\pi v |m|^2 \left(\frac{1}{2K} + C_2 |m|^{2(x_T-2)}\right), \tag{3.52}$$

where $1/N \propto m$ and m is replaced by $|m|$ as the system has the spin reversal symmetry $m \to -m$. In addition, for the sine-Gordon model, $C_1 = 0$, $x_T > 2$ [16], and $C_2 < 0$ [18]. We then consider $\epsilon^{(4)}(N, m)$ at $x_T > 2$ for the sine-Gordon model. In the thermodynamic limit, $\epsilon^{(2)}(N, m)$ in Eq. (3.10) is equal to $\chi^{-1}(m) = \epsilon''(m) = \frac{\partial^2 \epsilon(m)}{\partial m^2}$ which is analytic function. Thus, the second differential $\epsilon^{(2)}(N, m)$ are written by

$$\epsilon^{(2)}(N, m) = \frac{\partial^2 \epsilon(m)}{\partial m^2} = \frac{\partial^2}{\partial m^2}\frac{\Delta E}{N}$$
$$= 2\pi v \left\{\frac{2}{2K} + C_2(2x_T - 2)(2x_T - 3)|m|^{2(x_T-2)}\right\}. \tag{3.53}$$

Similarly, $\epsilon^{(4)}(N, m)$ is equivalent to $A(m) = \epsilon^{(4)}(m) = \frac{\partial^4 \epsilon(m)}{\partial m^4}$ in the thermodynamic limit. The fourth differential $\epsilon^{(4)}(N, m)$ is then written in the form

$$\epsilon^{(4)}(N, m) = 2\pi v C_2(2x_T - 2)(2x_T - 3)(2x_T - 4)(2x_T - 5)|m|^{2(x_T-3)}. \tag{3.54}$$

$\epsilon^{(4)}(N, m)$ diverges for $2 < x_T < 3$, i.e., $1/2 < \Delta < 1$ in the thermodynamic limit. $\epsilon^{(4)}(N, m) = 0$ at $x_T = 5/2$ and the case in which $\epsilon(m)$ is not analytic are left for future works as few investigations have been done. Next, we focus on the size dependence of $\epsilon^{(4)}(N, m = 0)$. We extend Eq. (3.52) in the form

$$E(N, M) - 2E(N, 0) + E(N, -M)$$
$$= 2\left[E(N, M) - E(N, 0)\right]$$
$$= \frac{4\pi v |M|^2}{N}\left\{\frac{1}{2K} + C_2\left|\frac{M}{N}\right|^{2(x_T-2)}\right\}, \tag{3.55}$$

where $|M| \ll N$ and $E(N, M) = E(N, -M)$. Using the above relation, the fourth differential in Eq. (3.11) is given by

$$\epsilon^{(4)}(N, m = 0)$$
$$= N^3\{E(N, 2) - 2E(N, 0) + E(N, -2) - 4(E(N, 1) - 2E(N, 0) + E(N, -1))\}$$
$$= 16\pi v C_2(2^{2(x_T-2)} - 1)N^{6-2x_T}, \tag{3.56}$$

where the coefficient $16\pi v C_2(2^{2(x_T-2)}-1)$ is a negative value for $C_2 < 0$ and $x_T > 2$. Thus, $\epsilon^{(4)}(N, m=0)$ diverges for $2 < x_T < 3$ in the thermodynamic limit.

Next, for $x_T = 2$, that is, $\Delta = 1$, we describe $\epsilon^{(4)}(N, m)$. The energy gap ΔE for a finite system size N is written as [20]

$$\Delta E = \frac{2\pi v}{N}\frac{1}{2}\left(1 - \frac{1}{2}\frac{1}{\ln \frac{N}{N_0}} + \frac{1}{4}\frac{\ln\left(\ln \frac{N}{N_0}\right)}{\left(\ln \frac{N}{N_0}\right)^2}\right), \tag{3.57}$$

where N_0 is a non-universal renormalization constant. The size dependence of $\epsilon^{(4)}(N, m=0)$ is discussed. We then extend Eq. (3.57) in the form

$$\begin{aligned} &E(N, M) - 2E(N, 0) + E(N, -M) \\ &= \frac{2\pi v}{N}|M|^2\left(1 - \frac{1}{2}\frac{1}{\ln \frac{N}{N_0|M|}} + \frac{1}{4}\frac{\ln(\ln \frac{N}{N_0|M|})}{(\ln \frac{N}{N_0|M|})^2}\right), \end{aligned} \tag{3.58}$$

where $E(N, M) = E(N, -M)$. Using this relation, the fourth differential $\epsilon^{(4)}(N, m)$ is given by

$$\begin{aligned} &\epsilon^{(4)}(N, m=0) \\ &= -4\pi v N^2 \left(\ln \frac{N}{N_0}\right)^{-2} \ln 2 \\ &\times \left(1 - \frac{\ln(\ln \frac{N}{N_0}) - \ln 2 - 1/2}{\ln \frac{N}{N_0}} + \mathcal{O}\left(\left(\ln \frac{N}{N_0}\right)^{-2}\right)\right). \end{aligned} \tag{3.59}$$

Therefore, $\epsilon^{(4)}(N, m=0)$ diverges in the thermodynamic limit. The finite m cases are left for future works.

These facts indicate the behavior of magnetic susceptibility χ and fourth derivative A, which is influenced by scaling dimension x_T. For the sine-Gordon model corresponding to $S = 1/2$ XXZ chain, that of χ and A depends on the change of scaling dimension which is related to a phase transition.

Chapter 4

Results

In this chapter, we describe the numerical results of magnetic susceptibility and fourth derivative.

4.1 Setup of system

To consider the anomaly, we calculate magnetic susceptibility χ and fourth derivative A, using the lowest energy $E(N, M)$. In order to calculate them, we use numerical diagonalization based on Lanczos method by TITPACK Ver.2 [21] and $H\phi$ [22]. Lanczos method is described in Appendix A. For example, we give $S = 1/2$ XXZ antiferromagnetic spin chain

$$\hat{\mathscr{H}} = J\sum_{j=1}^{N}(\hat{S}_j^x\hat{S}_{j+1}^x + \hat{S}_j^y\hat{S}_{j+1}^y + \Delta\hat{S}_j^z\hat{S}_{j+1}^z), \tag{4.1}$$

where $\hat{S}_j^x, \hat{S}_j^y, \hat{S}_j^z$ are the jth site spin operator in the x, y, z direction, Δ is an anisotropic parameter, N is the system size that is even from 10 to 26, and $J = 1$ is an exchange interaction. The definition of J in Eq. (4.1) is different from that of J in Chapter 2. The change of the phase is described by Δ, which shows ferromagnetic phase for $\Delta \leq -1$, Tomonaga–Luttinger phase for $-1 < \Delta \leq 1$, and antiferromagnetic phase for $\Delta > 1$ (Fig. 4.1). The boundary condition of the chain is periodic:

$$\hat{S}_{N+1} = \hat{S}_1. \tag{4.2}$$

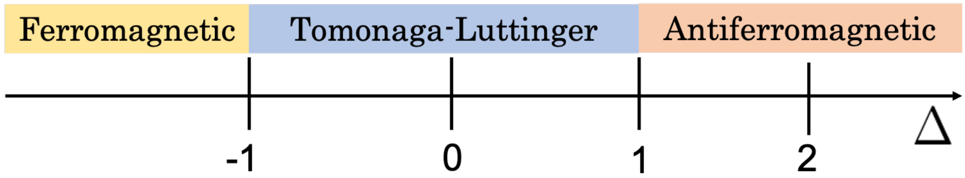

Fig. 4.1: Change of phase of $S = 1/2$ XXZ antiferromagnetic chain with parameter Δ, which shows ferromagnetic phase for $\Delta \leq -1$, Tomonaga–Luttinger phase for $-1 < \Delta \leq 1$, and antiferromagnetic phase for $\Delta > 1$.

4.2 $S = 1/2$ XXZ antiferromagnetic chain

The $S = 1/2$ XXZ antiferromagnetic chain (4.1) is solved by Bethe ansatz. The ground-state properties are well known for the chain [23, 24, 10, 25]. We introduce these properties. First, for $\Delta > 1$, the ground state of the chain shows antiferromagnetic long distance order and has double degeneracy for infinite systems.

Next, for $\Delta = 1$, the ground state describes disorder and no degeneracy. The correlation function is written as follows

$$\langle \hat{S}_i^\alpha \hat{S}_j^\alpha \rangle \simeq \frac{(-1)^{i-j}(\ln|i-j|)^{\frac{1}{2}}}{|i-j|}, \quad (\alpha = x, y, z) \tag{4.3}$$

where $i - j \gg 1$.

Next, for $|\Delta| < 1$, the ground state with disorder exists. The correlation function of spin is written in the form

$$\langle \hat{S}_i^x \hat{S}_j^x \rangle \simeq \frac{(-1)^{i-j}}{|i-j|^\eta}, \quad (i - j \gg 1) \tag{4.4}$$

$$\eta = \frac{1}{2} + \frac{1}{\pi} \arcsin \Delta, \tag{4.5}$$

where $0 < \eta < 1$ for $-1 < \Delta < 1$. The correlation function for $\hat{S}^z$ is given by

$$\langle \hat{S}_i^z \hat{S}_j^z \rangle \simeq \frac{(-1)^{i-j}}{|i-j|^{\frac{1}{\eta}}}. \tag{4.6}$$

As $\eta < 1$, the correlation function for $\hat{S}^z$ becomes small. Thus, the correlation function of $\hat{S}^x$ is dominant.

Finally, for $\Delta < -1$, the ground state has ferromagnetic long distance order and double degeneracy.

4.3 Numerical results

In this section, we show our numerical results for $\Delta = 0, 1, 2$ with several sizes from 10 to 20.

4.3.1 Magnetic susceptibility

First, we show the results of magnetic susceptibility χ. Figure 4.2 illustrates the magnetization dependence of χ. Figures 4.2(a) and 4.2(b) show smooth curves. Figure 4.2(c) shows a sharp cusp at zero magnetization. However, this cusp does not indicate an anomaly as an anomaly must satisfy the following conditions:

1. Magnetic susceptibility χ, χ^{-1}, and fourth derivative A have a cusp.

2. Size dependence of the cusp is large in the thermodynamic limit.

Thus, it is confirmed that Figure 4.2(c) does not have the anomaly as the size dependence is small. Similarly, neither Fig. 4.2(a) nor Fig. 4.2(b) shows the anomaly. These results mean that the anomaly of χ is not shown.

Next, we show the results of inverse of magnetic susceptibility χ^{-1}. Figure 4.3 illustrates the magnetization dependence of χ^{-1}. Figure 4.3(a) has no cusp, thus it does not show an anomaly. Figures 4.3(b) and 4.3(c) have sharp cusps at zero magnetization in comparison to Fig. 4.2. Thus, it is clearer to observe the cusp of χ^{-1} than of χ. However, Fig. 4.3(b) does not show an anomaly as the size dependence is small at zero magnetization. In contrast, Fig. 4.3(c) demonstrates that there is the possibility of showing an anomaly because the size dependence is large. These results indicate a possibility that χ^{-1} shows an anomaly for $\Delta > 1$ in the thermodynamic limit. The analysis of possibility of showing an anomaly is discussed later.

4.3.2 Fourth derivative

We show the results of fourth derivative A. Figure 4.4 illustrates the magnetization dependence of A. This indicates a decrease in A when the magnetization $m \to 0$ for $0 \leq \Delta \leq 1$. Figure 4.4(a) has no cusp, thus this does not show an anomaly. Figures 4.4(b) and 4.4(c) show sharp cusps at zero magnetization, compared with Fig. 4.3. In addition, Fig. 4.4(b) and 4.4(c) indicate the possibility of showing an anomaly because its size dependence is large. These results show that it is clearer to observe the possibility of an anomaly by A than by χ^{-1}. The difference between Fig. 4.4(b) and Fig. 4.4(c) is the behavior of $m = \pm 1/N$. Figure 4.4(b) shows negative values at $m = \pm 1/N$. Although A in Fig. 4.4(b) seems to be discontinuous near $m = 0.1$, this behavior is superficial. Actually, the analysis of

Fig. 4.4(b) leads to Fig. 4.5. Figure 4.5 illustrates the A for three system sizes: 10, 14, and 20. This indicates that A is continuous near $m = 0.1$. Therefore, A near $m = 0.1$ is continuous for $\Delta = 1$. While Fig. 4.4(b) shows negative values at $m = \pm 1/N$, Fig. 4.4(c) shows large positive values at $m = \pm 1/N$. These behaviors of A at $m = 0, 1/N$ indicate that there is the possibility of showing an anomaly for $\Delta > 1$ as its size dependence is large. This is explained by Eq. (3.16). However, we do not know the behavior of A for $\Delta < 1$ and $N \to \infty$. These details are discussed later.

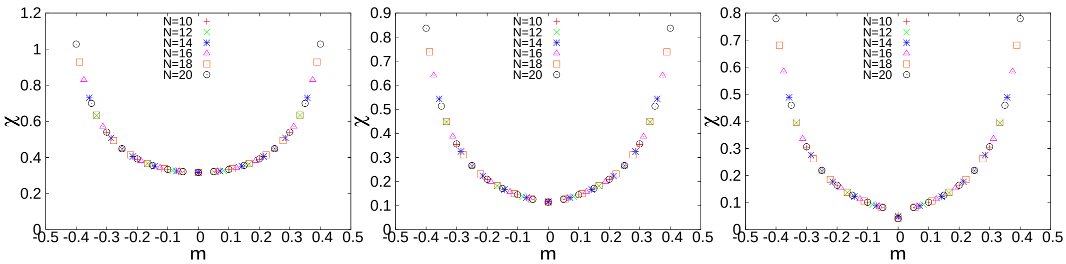

(a) $\Delta = 0$ **(b)** $\Delta = 1$ **(c)** $\Delta = 2$

Fig. 4.2: Magnetization m dependence of the magnetic susceptibility χ of the $S = 1/2$ XXZ antiferromagnetic chain for several system sizes N: 10, 12, 14, 16, 18, and 20. Both panels (a) and (b) indicate that χ has smooth curves. Conversely, panel (c) shows that the χ has a sharp cusp at $m = 0$. However, for panel (c), an anomaly of χ is not shown because the size dependence is small. Thus, χ does not show an anomaly.

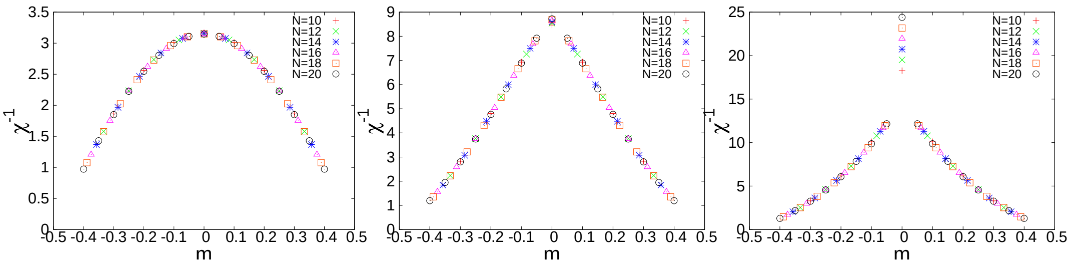

(a) $\Delta = 0$ **(b)** $\Delta = 1$ **(c)** $\Delta = 2$

Fig. 4.3: Magnetization m dependence of the inverse of the magnetic susceptibility χ^{-1} of the $S = 1/2$ XXZ antiferromagnetic chain for several system sizes N: 10, 12, 14, 16, 18, and 20. Panel (a) demonstrates that χ^{-1} indicates smooth curve and does not show a cusp. Conversely, panel (b) demonstrates that χ^{-1} shows a cusp and a low size dependence at $m = 0$. Panel (c) demonstrates that χ^{-1} shows a sharp cusp of large positive values and high size dependence at $m = 0$ in comparison to panel (b). Therefore, it is easier to observe the cusp of χ^{-1} than that of χ in Fig. 4.2. Moreover, it is possible for χ^{-1} to show an anomaly for $\Delta > 1$ owing to its high size dependence at $m = 0$.

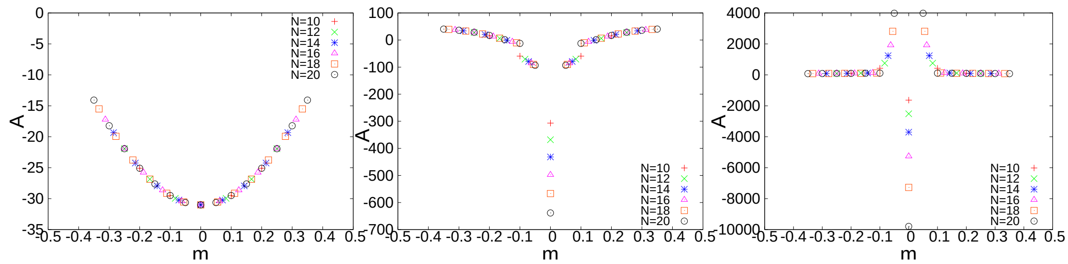

(a) $\Delta = 0$ **(b)** $\Delta = 1$ **(c)** $\Delta = 2$

Fig. 4.4: Magnetization m dependence of the fourth derivative A of the $S = 1/2$ XXZ antiferromagnetic chain for several system sizes N: 10, 12, 14, 16, 18, and 20. Panel (a) demonstrates that A shows smooth curve and does not show a cusp. In contrast, both panels (b) and (c) demonstrates that A shows a sharp cusp of large negative values and a high size dependence at $m = 0$. Moreover, for panel (c), A has large positive values and a high size dependence at $m = \pm 1/N$. Therefore, it is possible for A to show an anomaly for $\Delta \geq 1$ owing to its high size dependence at zero magnetization.

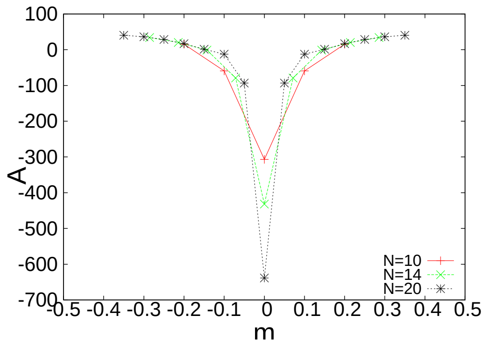

Fig. 4.5: Magnetization m dependence of the fourth derivative A for $\Delta = 1$ for three system sizes: 10, 14, and 20. A has a continuous curve, compared with Fig. 4.4(b).

Chapter 5

Comparison with exact solutions

In this chapter, our numerical results are compared with exact solutions [26, 27, 28, 20, 29] for investigating the behavior of A. The behavior of χ is well established for all Δ. However, few investigations of the behavior of A have previously been carried out. We indicate that the reliability of the results of A increases when the results of χ are consistent with exact solutions. This is useful to study the behavior of A.

5.1 Magnetic susceptibility near saturation magnetization

The spin S Heisenberg antiferromagnetic chain is defined as

$$\hat{\mathscr{H}} = J\sum_{j=1}^{N}(\hat{S}_j^x\hat{S}_{j+1}^x + \hat{S}_j^y\hat{S}_{j+1}^y + \hat{S}_j^z\hat{S}_{j+1}^z) - h\sum_{j=1}^{N}\hat{S}_j^z, \tag{5.1}$$

where J is an exchange interaction and positive, $\hat{S}_j^x, \hat{S}_j^y, \hat{S}_j^z$ are the jth site spin operator in the x, y, z direction, N is the system size, and h is a magnetic field. We then consider the magnetic susceptibility near saturation magnetization. First, a ground state energy g of the chain per site is given by [30, 31]

$$g(T, h, S) = (JS^2 - hS) + JSf\left(\frac{T}{JS}, 4 - \frac{h}{JS}, \frac{2}{S}\right), \tag{5.2}$$

where T, h, and f are temperature, magnetic field, and ground state energy of $\hat{\mathscr{H}_z} = -h\sum_j \hat{S}_j^z$ per site respectively. At $T = 0$ and near saturation magnetization, f is written in the form [30, 31, 32]

$$f\left(T = 0, 4 - \frac{h}{JS}, \frac{2}{S}\right) = -\frac{2}{3\pi}\left(4 - \frac{h}{JS}\right)^{3/2}. \tag{5.3}$$

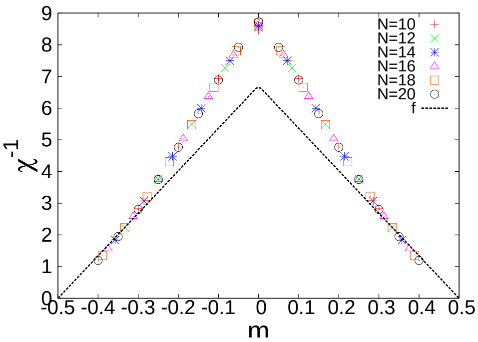

Fig. 5.1: Magnetization m dependence of the inverse of the magnetic susceptibility χ^{-1} for $\Delta = 1$. f is the fitting function expressed by Eq. (5.7). Our numerical results are consistent with f near saturation magnetization.

The ground state energy g, magnetization m, and magnetic susceptibility χ are then obtained by

$$g(0, h, S) = S^2 - hS - \frac{2S}{3\pi}\left(4 - \frac{h}{S}\right)^{3/2}, \tag{5.4}$$

$$m = -\frac{\partial g}{\partial h} = S - \frac{1}{\pi}\left(4 - \frac{h}{S}\right)^{1/2}, \tag{5.5}$$

$$\chi = \frac{\partial m}{\partial h} = \frac{1}{2\pi S}\left(4 - \frac{h}{S}\right)^{-1/2}, \tag{5.6}$$

where $J = 1$. Thus, the inverse of magnetic susceptibility χ^{-1} is proportional to the magnetization $S - m$ near the saturation magnetization. In our case that is $S = 1/2$, the magnetic susceptibility is written as

$$\chi^{-1} \propto 1/2 - m. \tag{5.7}$$

We indicate that our numerical results are consistent with Eq. (5.7). Figure 5.1 shows a magnetization dependence of χ^{-1} for $\Delta = 1$ with a fitting function f that is described by Eq. (5.7). The fitting is carried out in $0.3 \leq |m| \leq 0.4$. From the graph, there is a linear relation between χ^{-1} and m near saturation magnetization ($m = 1/2$) because f is consistent with our results. However, the linear relation is applicable only to the points where f is consistent with our results. Thus, our results of χ are reliable, and the reliability of our results of A increases.

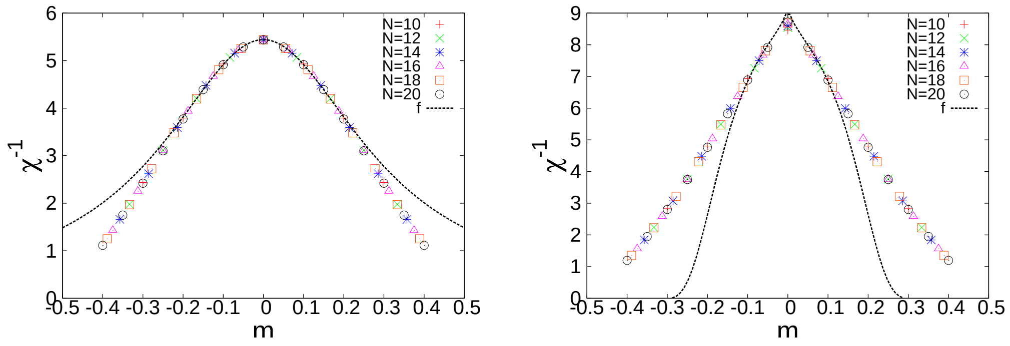

Fig. 5.2: Magnetization m dependence of the inverse of the magnetic susceptibility χ^{-1} with a fitting function f. Panel (a) indicates that f is expressed by the inverse of Eq. (5.10). Panel (b) indicates that f is expressed by the inverse of Eq. (5.13). Our numerical results are consistent with f under $0 < |m| \leq 0.1$.

5.2 Bethe-ansatz solution

The Bethe ansatz is an exact method applied in a wide range of fields, such as quantum field theory and statistical mechanics. We compare our numerical results with exact solutions.

5.2.1 Case of magnetic susceptibility near zero magnetization

First, under $0 < \Delta < 1$, we consider $S = 1/2$ XXZ antiferromagnetic chain (5.1). The exact solution of χ is then given by [23]

$$\chi = \frac{4\gamma}{\pi(\pi - \gamma)\sin\gamma}\{1 + \mathcal{O}(h^2) + \mathcal{O}(h^{\frac{4\gamma}{\pi-\gamma}})\}, \tag{5.8}$$

$$\gamma = \arccos\Delta. \tag{5.9}$$

As it is difficult to compare our numerical results with Eq. (5.8), we rewrite Eq. (5.8) as a function of m in the following way

$$\chi = \frac{4\gamma}{\pi(\pi - \gamma)\sin\gamma} + c_1 m^2 + c_2 |m|^{\frac{4\gamma}{\pi-\gamma}}, \tag{5.10}$$

$$h = \frac{4\gamma}{\pi(\pi - \gamma)\sin\gamma} m,$$

$$c_1 = \frac{a}{16\pi\beta^2}\frac{\kappa}{2}\left(\frac{4}{\beta^2} - 2\right)\left(\frac{4}{\beta^2} - 3\right),$$

$$c_2 = \frac{3a^2}{8\pi\beta^2}(\kappa_+ + \kappa_-),$$

where c_1 and c_2 are derived from Eq. (2.57), $a > 0$ and $0 < \beta^2 \leq 1$, and κ, κ_+, κ_- are written as

$$\kappa = \frac{\Gamma^2\left(\beta^{-2}\right)\tan\left(\pi\beta^{-2}\right)}{2\beta^2\Gamma^2\left(\frac{1}{2}+\beta^{-2}\right)}\left[\frac{\Gamma\left(\frac{\beta^2}{2-2\beta^2}\right)}{8\sqrt{\pi}\Gamma\left(\frac{1}{2-2\beta^2}\right)}\right]^{\frac{2}{\beta^2}-2},$$

$$\kappa_+ = \frac{1}{64\pi\beta^2}\tan\left(\frac{\pi}{2-2\beta^2}\right),$$

$$\kappa_- = \frac{1}{192\pi}\frac{\Gamma\left(\frac{3}{2-2\beta^2}\right)\Gamma^3\left(\frac{\beta^2}{2-2\beta^2}\right)}{\Gamma\left(\frac{3\beta^2}{2-2\beta^2}\right)\Gamma^3\left(\frac{1}{2-2\beta^2}\right)}.$$

Eq. (5.10) is consistent with Eq. (3.53). We then perform the fitting with Eq. (5.10) under $0 < |m| \leq 0.1$. The result is shown in Fig. 5.2(a). Figure 5.2(a) indicates that our results are consistent with exact solutions near zero magnetization. Therefore, this consistency increases the reliability of our numerical results of χ for $0 < \Delta < 1$.

Next, we explain the exact solution of χ for $\Delta = 1$. In this case, although it appears that $h^{\frac{4\gamma}{\pi-\gamma}} = h^0$ from Eq. (5.8), there remains a possibility of logarithmic behavior from the solutions of a Hubbard model [33]. The Hubbard model is regarded as an isotropic Heisenberg model with an infinite Coulomb repulsion. Thus, using the exact solution of the Hubbard model, that of χ is given by [33]

$$\frac{\chi}{\chi_0} = 1 + \frac{1}{2}\frac{1}{\ln\frac{h_c}{h}\gamma_c} - \frac{1}{4}\frac{\ln\ln\frac{h_c}{h}\gamma_c}{(\ln\frac{h_c}{h}\gamma_c)^2} + \text{h.o.}, \tag{5.11}$$

$$h_c = 4\sin^2\left(\frac{\pi}{2}n\right), \gamma_c = \frac{\pi}{2}\sqrt{\frac{2\pi}{e}}, \tag{5.12}$$

where χ_0, n, and h.o. are the magnetic susceptibility at zero magnetization, a filling that denotes electron density, and high-order terms, respectively. For an isotropic Heisenberg model, n=1 and χ_0=$1/\pi^2$ [9, 34]. Similarly, we rewrite Eq. (5.11) as a function of m for the Heisenberg model

$$\chi = \frac{1}{\pi^2} + \frac{1}{2\pi^2}\frac{1}{\ln\frac{2\pi\sqrt{\frac{2\pi}{e}}}{d_0 m}} - \frac{1}{4\pi^2}\frac{\ln\ln\frac{2\pi\sqrt{\frac{2\pi}{e}}}{d_0 m}}{\left(\ln\frac{2\pi\sqrt{\frac{2\pi}{e}}}{d_0 m}\right)^2}, \tag{5.13}$$

$$h = d_0 m,$$

where d_0 is a constant. We perform the fitting with Eq. (5.13) under $0 \leq |m| \leq 0.1$. The result is shown in Fig. 5.2(b). Figure 5.2(b) indicates that our results

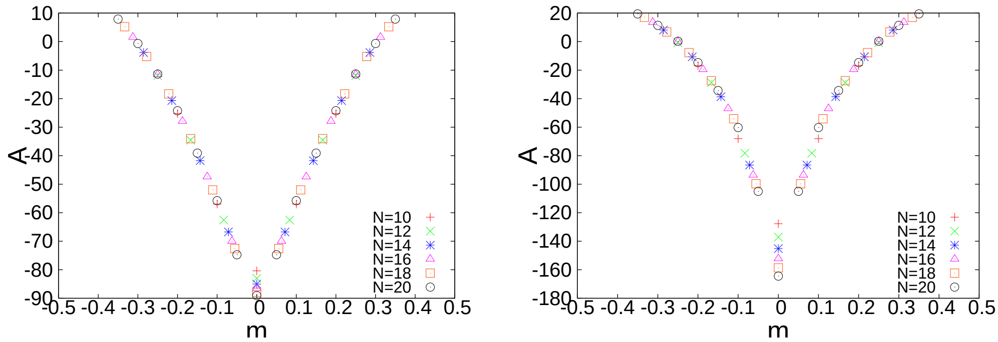

(a) $\Delta = 0.4$ **(b)** $\Delta = 0.6$

Fig. 5.3: Magnetization m dependence of the fourth derivative A near $\Delta = 1/2$. Panel (a) indicates that A seems to be finite as its size dependence is small when $m \to 0$. Panel (b) shows that A appears to be infinite when as its size dependence is large when $m \to 0$. Our numerical results are consistent with Eq. (5.16) and Eq. (5.17).

are consistent with exact solutions near zero magnetization. Thus, our results are consistent with exact solutions in $0 < \Delta \leq 1$. This indicates that the reliability of the results of A increases with that of χ. However, for $\Delta = 1$ the magnetic susceptibility shows an infinite slope when m approaches zero from Griffiths's theory [9]. The cause of the differences between the theoretical and calculated results is a finite size effect.

5.2.2 Case of fourth derivative

The exact solutions of A have not been investigated. However, for $-1 < \Delta < 1$, C.N. Yang and C.P. Yang discussed [12, 13]

$$\lim_{m\to 0+} \frac{\mathrm{d}^n \chi^{-1}}{\mathrm{d}m^n} = \begin{cases} \text{finite} & \left(n < \dfrac{4\mu}{\pi - \mu}\right), & (5.14) \\ \text{infinite} & \left(n > \dfrac{4\mu}{\pi - \mu}\right), & (5.15) \end{cases}$$

where $\mu = \arccos \Delta$. In the case of $n = 2$, the condition of (5.14) is

$$\begin{aligned} 2 &< \frac{4 \arccos \Delta}{\pi - \arccos \Delta} \\ \frac{\pi}{3} &> \arccos \Delta \\ \frac{1}{2} &> \Delta. \end{aligned}$$

Similarly, the condition of Eq. (5.15) is $\Delta > \frac{1}{2}$. Thus, the relations of fourth derivative A are shown in the following way

$$\lim_{m\to 0+} A = \begin{cases} \text{finite} & (-1 < \Delta < 1/2), & (5.16) \\ \text{infinite} & (1/2 < \Delta < 1). & (5.17) \end{cases}$$

The numerical results of A are shown in Fig. 5.3. Figure 5.3(a) indicates that A becomes finite as m approaches zero because its size dependence is small. In contrast, Fig. 5.3(b) indicates that A appears to become infinite as m approaches zero from of its large size dependence. Thus, our results are explained by the tendency of the exact solutions. $\Delta = 1/2$ corresponds to $N = 2$ supersymmetry (SUSY) in a conformal field theory [35]. Details of this are discussed in a later chapter.

Chapter 6

Discussion

In this chapter, we investigate the anomalies of χ^{-1} and A at $m = 0$ for $0 \leq \Delta \leq 2$ from the perspective of size dependence. In addition, from the behavior at $m = 1/N$ in Fig. 4.4(b) and Fig. 4.4(c), we investigate the anomalies of χ^{-1} and A at $m = 1/N$. In particular, from scaling dimension which indicates the critical exponent, we analyze the anomaly of A at $\Delta = 1/2$. We study the anomaly of the third derivative associated with non-linear magnetic susceptibility [36].

6.1 Anomaly of $\Delta = 1/2$

We focus on the point $\Delta = 1/2$ of $S = 1/2$ XXZ antiferromagnetic chain from Eq. (5.16) and Eq. (5.17). We describe the relationship between the anomaly of A, scaling dimension, and phase transition.

6.1.1 Scaling dimension

From previous chapter, we demonstrate that the $\Delta = 1/2$ point corresponds to the $N = 2$ SUSY for a conformal field theory (CFT). We apply CFT to the $S = 1/2$ XXZ antiferromagnetic chain. The anisotropic parameter of the chain Δ is related to the scaling dimension x_T, which indicates the critical exponent [37]. It is shown for $-1 < \Delta \leq 1$ that [18, 24]

$$x_T(k = 0) = \frac{2\pi}{\arccos(-\Delta)}, \tag{6.1}$$

where k is the wavenumber of the spin state that is a parameter obtained from translational symmetry. We focus on the scaling dimension with the wavenumber $k = 0$ and zero magnetization, as it is compatible with the symmetry of the Hamiltonian. For $\Delta = 1/2$, from Eq. (6.1), $x_T(k = 0) = 3$. The scaling dimensions $x_T(k = 0) > 2$ show the irrelevant characteristics [37]. Thus, $x_T(k = 0) = 3$ shows the irrelevant characteristics. S.K. Yang [38] demonstrated that $x_T(k = 0) = 3$ corresponds to $N = 2$ SUSY from the correspondence between the XXZ chain and Ashkin–Teller model. Furthermore, P. Ginsparg [35] and Luther and Peschel [24] showed the correspondence table between the scaling dimension, XXZ chain, and free boson model. Therefore, these discussions show that $\Delta = 1/2$ corresponds to $N = 2$ SUSY.

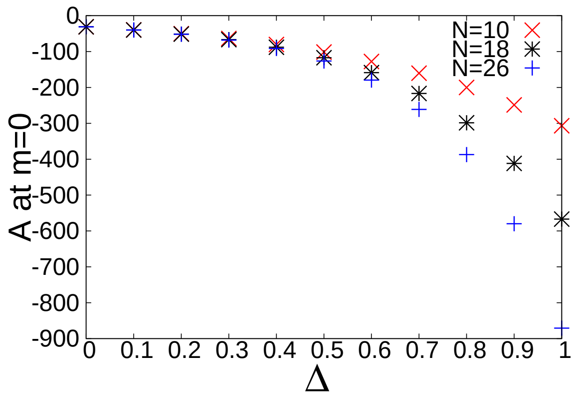

Fig. 6.1: Anisotropic parameter Δ dependence of the fourth derivative A at zero magnetization for several system sizes N: 10, 18, and 26. The A appears to diverge for $\Delta > 1/2$ as the size dependence is large. Thus, the starting point of the anomaly of A is the $\Delta = 1/2$ point. The origin of the anomaly of A at $1/2 < \Delta < 1$ does not indicate the phase transition from the scaling dimension [39]. The $-1 < \Delta < 1/2$ region is named TL phase (I) and $1/2 < \Delta \leq 1$ is named TL phase (II) based on the behavior of A. Thus, the origin of the anomaly of A at $1/2 < \Delta < 1$ is TL phase (II).

6.1.2 Scaling dimension and the anomaly

We analyze the anomaly of $\Delta = 1/2$ and the origin of that from the scaling dimension x_T. First, we consider the $\Delta = 1/2$ point treated in previous section. Figure 6.1 indicates the Δ dependence of the fourth derivative A at zero magnetization. It appears that A diverges for $\Delta > 1/2$ as the size dependence is large, thus A at $1/2 < \Delta < 1$ shows the anomaly. This is as expected by C.N. Yang and C.P. Yang [12, 13]. We then consider the origin of the anomaly from the perspective of the scaling dimension x_T subject to the parameter Δ [12, 23]. For $\Delta = 1$, the scaling dimension x_T changes from irrelevant to relevant for $U(1)$ symmetry.

This change of the scaling dimension means the phase transition corresponding to the Kosterlitz–Thouless (KT) transition. In contrast, for $-1 < \Delta \leq 1$ region that shows Tomonaga–Luttinger (TL) phase, the scaling dimension x_T is irrelevant. For $\Delta = 2$ region that shows the antiferromagnetic phase, the scaling dimension x_T is relevant in $\Delta > 1$ [24]. Thus, the origin of the anomaly of A at $1/2 < \Delta < 1$ is not phase transition. These indicate that the anomaly of A is analyzed from the perspective of the scaling dimension x_T. In addition, from the behavior of A at $1/2 < \Delta < 1$, we reveal that Tomonaga–Luttinger (TL) phase is divided into two phases with a $\Delta = 1/2$ boundary. We name $-1 < \Delta < 1/2$ TL phase (I) and $1/2 < \Delta \leq 1$ TL phase (II). Therefore, the origin of the anomaly of A at $1/2 < \Delta < 1$ is TL phase (II).

6.2 Analysis of anomalies

We investigate the anomalies of high-order derivative such as χ, fourth derivative A, and third derivative D.

6.2.1 Magnetic susceptibility

The behaviors of χ and χ^{-1} are shown at zero magnetization in Fig. 6.2. Figure 6.2(a) shows that χ^{-1} becomes finite for $\Delta = 1$ in the thermodynamic limit. This indicates that the system does not have a finite spin gap and an anomaly. In contrast, Fig. 6.2(b) shows that χ^{-1} becomes infinite, i.e., χ reaches zero for $\Delta = 2$ in the thermodynamic limit. However, it is not conclusive that χ approaches zero in the thermodynamic limit. To solve this problem, we present Fig. 6.2(c). Figure 6.2(c) shows that χ^{-1} becomes infinite in the thermodynamic limit. Thus, χ for $\Delta = 2$ approaches zero. This indicates that the system has a finite spin gap and an anomaly for $\Delta = 2$. The origin of the anomaly is a Neel state that is double degeneracy of the ground state with energy gap. These facts are consistent with the results obtained by C.N. Yang and C.P. Yang; [12, 13] thus, we observed an anomaly of the magnetic susceptibility in a one-dimensional system. Moreover, the observation of the anomaly of that is useful for distinguishing gapped from gapless systems.

6.2.2 Fourth derivative

The behavior of A at zero magnetization is shown in Fig. 6.3. Figure 6.3(a) shows that A becomes finite for $\Delta = 0.3$ in the thermodynamic limit, whereas Fig. 6.3(b) shows that it is negative infinity for $\Delta = 0.7$ in the thermodynamic limit. For $\Delta = 0.7$, from Eq. (3.56), A is proportional to $N^{6-2x_T} = N^{0.6439}$, as

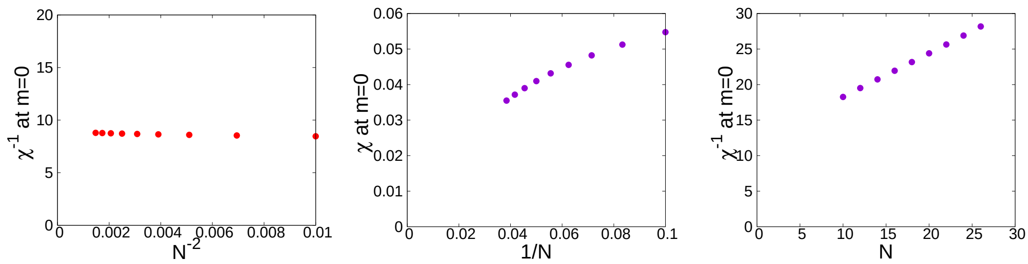

(a) $\Delta = 1$ **(b)** $\Delta = 2$ **(c)** $\Delta = 2$

Fig. 6.2: N dependence of the magnetic susceptibility χ and its inverse χ^{-1} at zero magnetization. Closed circles denote values of the magnetic susceptibility for several system sizes N: 10, 12, 14, 16, 18, 20, 22, 24, and 26. Panel (a) demonstrates that χ^{-1} becomes finite in the thermodynamic limit. Panel (c) demonstrates that χ^{-1} approaches infinity in the thermodynamic limit. Therefore, panel (b) demonstrates that χ approaches zero in the thermodynamic limit and shows an anomaly that is a Neel state which is double degeneracy of the ground state with energy gap.

the scaling dimension $x_T = 2.678003$ in Eq. (6.1). Thus, we plot the horizontal axis in Fig. 6.3(b) as $N^{-0.644}$. The behavior of A for $\Delta = 0.7$ is consistent with Eq. (3.56), in terms of both a power law and sign of the divergence. Both Fig. 6.3(c) and Fig. 6.3(d) show that A is negative infinity in the thermodynamic limit. For $\Delta = 1$, from Eq. (3.59), A is proportional to N^2. Thus, we plot the horizontal axis in Fig. 6.3(c) as N^{-2}. The behavior of A for $\Delta = 1$ is consistent with Eq. (3.59), in terms of both a power law and sign of the divergence. For $\Delta = 2$, from Eq. (3.16), A is proportional to N^3. Therefore, we plot the horizontal axis in Fig. 6.3(d) as N^{-3}. The behavior of A for $\Delta = 2$ is consistent with Eq. (3.16), in terms of both a power law and sign of the divergence. These results demonstrate that A shows an anomaly for $\Delta = 0.7, 1$, and 2. However, the origin of the anomaly is different. For $\Delta = 0.7$, the origin of the anomaly is TL phase (II). The origin of the anomaly for $\Delta = 1$ is the phase transition, which means the transition from TL liquid phase to antiferromagnetic phase [12, 23]. In contrast, in the $\Delta > 1$ region, a Neel state appears for the $S = 1/2$ XXZ antiferromagnetic chain. Thus, the origin of the anomaly for $\Delta = 2$ is the Neel state. Moreover, A shows the transition for $\Delta = 1$, although χ^{-1} does not show it from Fig. 6.2(a). The difference is used to confirm whether a phase transition happens or not. Therefore, observing A is helpful for determining the consistency of phase transition.

Next, we show A at $m = 1/N$ in Fig. 6.4, as the behavior of A at $m = 1/N$ differs between Fig. 4.4(b) and Fig. 4.4(c). Figure 6.4(a) shows that A becomes finite for $\Delta = 0.3$ in the thermodynamic limit, whereas Fig. 6.4(b) shows that it is minus infinity for $\Delta = 0.7$ in the thermodynamic limit. The behavior of A for

$\Delta = 0.7$ is consistent with Eq. (3.54). The origin of the anomaly is TL phase (I I). It appears that A in Fig. 6.4(c) becomes finite for $\Delta = 1$. However, when m approaches zero, the high-order differential of free energy becomes infinite from Eq. (2.26). Thus, A becomes infinite as the system size becomes larger in our calculation. The origin of the anomaly is phase transition. In contrast, Fig. 6.4(d) shows that A reaches infinity for $\Delta = 2$ in the thermodynamic limit. The behavior of A is consistent with Eq. (3.16). This indicates that A shows an anomaly for $\Delta = 2$. The origin of the anomaly is a Neel state. Therefore, the behavior of A at $m = 1/N$ is explained by Eq. (3.16) and Eq. (2.26). Observation of the change in behavior at $m = 1/N$ can be proposed as a new technique to distinguish gapped from gapless systems. Hence, observing A at $m = 1/N$ allows us to distinguish gapped from gapless systems. However, future works must focus on the exact solutions of A at $m = 1/N$, as few investigations have focused on this behavior.

These findings indicate that observation of A is more efficient than that of χ. Thus, we expect this technique to be used for analysis of spin liquids with spin gap issues in triangular and Kagome lattices [4, 5, 6, 7].

6.2.3 Third derivative

We discuss the third derivative involved in non-linear magnetic susceptibility [36]. The non-linear magnetic susceptibility with transformation between a magnetization and magnetic field is discussed in Appendix C. From Eq. (3.5), the third derivative is defined in the form

$$D \equiv \frac{\partial}{\partial m}\chi^{-1} = \frac{\partial^3}{\partial m^3}\epsilon(m). \tag{6.2}$$

The difference $\epsilon^{(3)}(N, m)$ between the lowest energies $E(N, M)$ is described by D as follows

$$\begin{aligned}
&\epsilon^{(3)}(N, m) \\
&\equiv \frac{N^2}{2}\{E(N, M+2) - 2E(N, M+1) + 2E(N, M-1) - E(N, M-2)\} \\
&= D + C^{(3)}(N, m) + \frac{1}{4N^2}(\epsilon^{(5)}(m) + C^{(5)}(N, m)) + \mathcal{O}\left(\frac{1}{N^4}\right),
\end{aligned} \tag{6.3}$$

where $\epsilon^{(n)}(N, m)$ is the nth finite-difference between the lowest energies. We then show numerical results of D in Fig. 6.5. The graph for $\Delta = 0$ in Fig. 6.5 shows that D and m appear to have a linear relation. The graph for $\Delta = 1/2$ in Fig. 6.5 indicates that D has smooth curves. However, D for $\Delta = 0$ and $1/2$ does nos show anomaly as there are no cusps. In contrast, Fig. 6.5 indicates that D for $\Delta = 1$ and 2 has a cusp at $m = 1/N$. Thus, the results show that there is possibility for showing anomaly for $\Delta = 1, 2$. From Eq. (5.14) and Eq. (5.15), the behaviors of D is given by

$$\lim_{m\to 0+} D = \lim_{m\to 0+} \frac{\partial \chi^{-1}}{\partial m} = \begin{cases} \text{finite} & \left(-1 < \Delta < \dfrac{1+\sqrt{5}}{4}\right), \quad (6.4) \\ \text{infinite} & \left(\dfrac{1+\sqrt{5}}{4} < \Delta < 1\right), \quad (6.5) \end{cases}$$

where $\frac{1+\sqrt{5}}{4} \simeq 0.81$. For $\Delta \gg 1$ in the thermodynamic limit, considering Eq. (3.12), we obtain

$$\epsilon^{(3)}(N, m) = \begin{cases} 0 & (m = 0), \\ N^2(-\Delta E) & (m = 1/N), \\ N^2(\Delta E) & (m = -1/N), \\ 0 & (m \neq 0, \pm 1/N), \end{cases} \tag{6.6}$$

where ΔE is an energy gap for a finite system. For a finite anisotropy and large N, as $\epsilon^{(3)}(N, m)$ is nonzero in $m \neq 0, \pm 1/N$, the above relation is changed in the form

$$\epsilon^{(3)}(N, m) = \begin{cases} 0 & (m = 0), \\ N^2(-\Delta E) & (m = 1/N), \\ N^2(\Delta E) & (m = -1/N), \\ finite & (m \neq 0, \pm 1/N). \end{cases} \tag{6.7}$$

Next, the behavior of D at $m = 1/N$ is shown in Fig. 6.6. The graph for $\Delta = 0$ and $1/2$ in Fig. 6.6 shows that D becomes finite in the thermodynamic limit. These analysis of size dependence are consistent with Eq. (6.4). In contrast, the graph for $\Delta = 1$ and $\Delta = 2$ indicates that D has negative infinity in the thermodynamic limit. The behavior of D for $\Delta = 1$ is expected by Griffiths [9] that showed infinite slope of the magnetic susceptibility. The origin of the anomaly is phase transition. Subsequently, the behavior of D for $\Delta = 2$ is consistent with Eq. (6.7), in terms of both a power law and sign of the divergence. The origin of the anomaly is a Neel state that is double degeneracy of the ground state with energy gap. These demonstrate that D shows anomaly for $\Delta = 1$ and 2.

6.3 Correction term and boundary conditions

The correction term of Eq. (3.5) changes in relation to boundary conditions and dimension. First, we discuss $C(N, m)$ in one-dimensional systems. Without anomaly, $C(N,m)$ in a periodic boundary condition is written in the conformal field theory as [40, 41, 42]

$$C(N,m) = -\frac{\pi v(m)}{6N^2}, \tag{6.8}$$

where $v(m)$ is the velocity of the spin wave and a smooth function for m. Thus, $\epsilon''(N,m)$ and $\epsilon^{(4)}(N,m)$ in Eq. (3.10) and Eq. (3.11) converges to $1/N^2$ order, which agrees with our numerical results. In contrast, the correction term for an open boundary is given by [40, 41, 42]

$$C(N,m) = \frac{b(m)}{N} - \frac{\pi v(m)}{24N^2}, \tag{6.9}$$

where $b(m)$ is a non-universal boundary term. In general, the convergence of this term is worse than that for a periodic boundary condition. We do not perform calculations for open boundary conditions herein, and leave them for future work.

Next, we discuss the correction term in two-dimensional systems. The correction term quickly converges, as shown by Nakano and Sakai [4], and thus, has convergence of at least second order. Unlike in the one-dimensional case, the convergence depends on the shape of the lattice. Figure 4 in Ref. [4] is different from Fig. 4.2(b) from the perspective of an energy gap, although it resembles Fig. 4.2(b) from previous research [4]. This problem will be addressed in our future works.

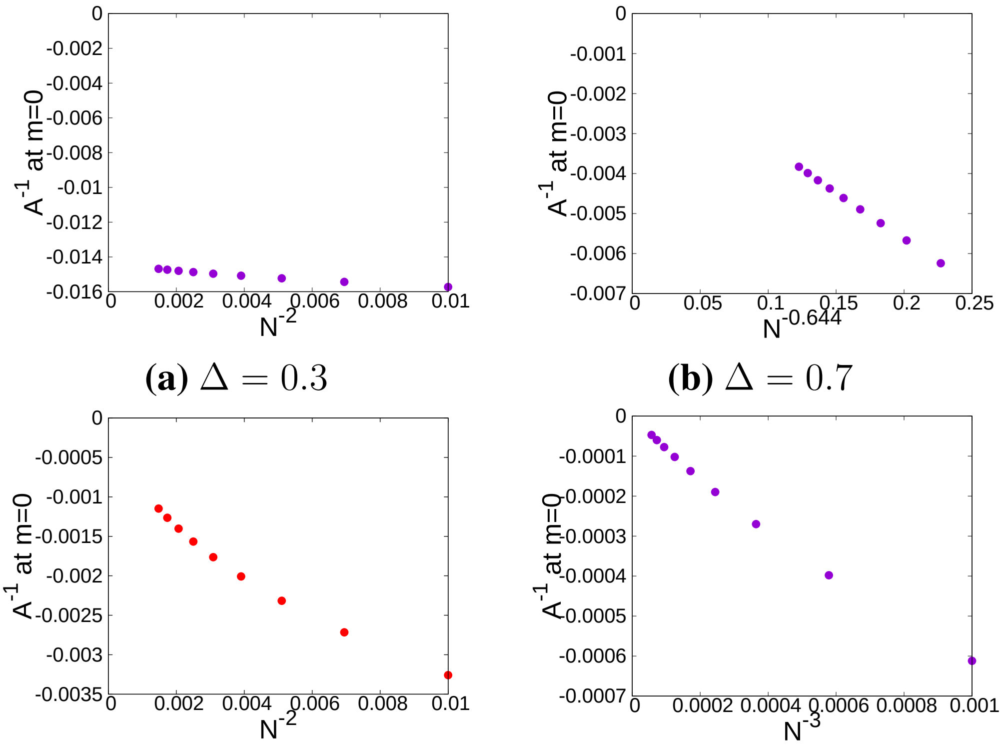

(a) $\Delta = 0.3$ **(b)** $\Delta = 0.7$

(c) $\Delta = 1$ **(d)** $\Delta = 2$

Fig. 6.3: N dependence of the fourth derivative A at zero magnetization. Closed circles denote values of A for several system sizes N: 10, 12, 14, 16, 18, 20, 22, 24, and 26. Panel (a) indicates that A becomes constant and does not show an anomaly in the thermodynamic limit. Panel (b) indicates that A approaches minus infinity and is consistent with Eq. (3.56) in the thermodynamic limit. Thus, panel (b) indicates an anomaly that shows TL phase (Ⅱ). Both panels (c) and (d) demonstrate that A becomes minus infinity in the thermodynamic limit. These numerical results for $\Delta = 1$ and $\Delta = 2$ are consistent with Eq. (3.59) and Eq. (3.16). Therefore, both panels (c) and (d) show an anomaly that indicates Kosterlitz–Thouless (KT) transition for $\Delta = 1$ and a Neel state that is double degeneracy of the ground state with energy gap for $\Delta = 2$.

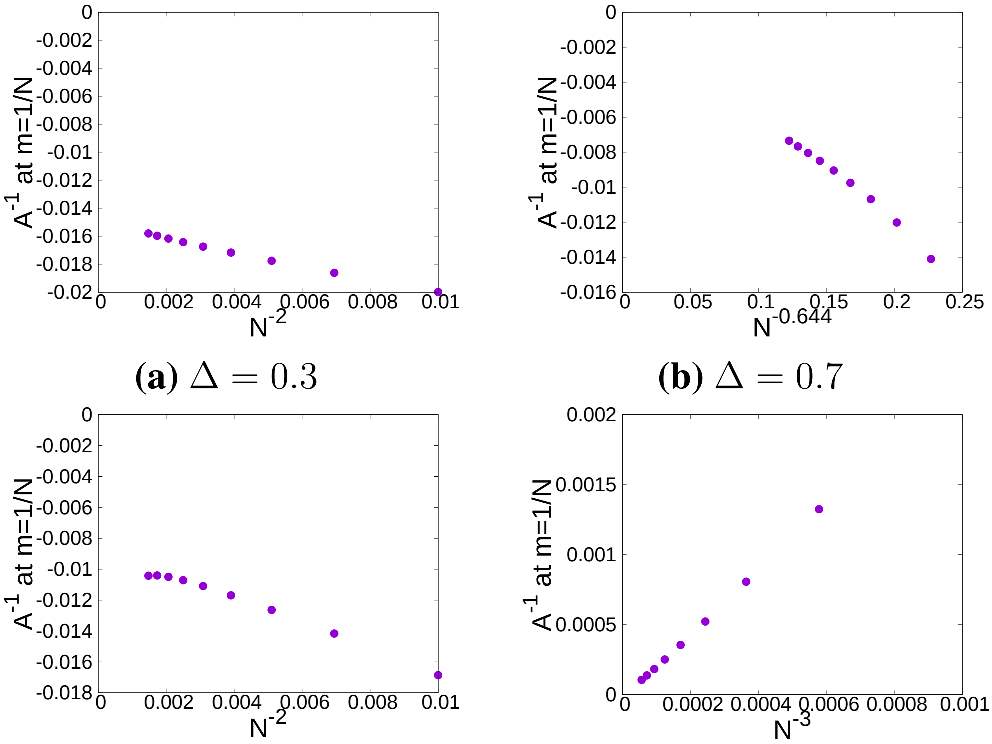

(a) $\Delta = 0.3$ **(b)** $\Delta = 0.7$ **(c)** $\Delta = 1$ **(d)** $\Delta = 2$

Fig. 6.4: N dependence of the fourth derivative A^{-1} at $m = 1/N$. Closed circles denote values of A for several system sizes N: 10, 12, 14, 16, 18, 20, 22, 24, and 26. Panel (a) indicates that A becomes finite does not show an anomaly in the thermodynamic limit. Panel (b) indicates that A approaches minus infinity and is consistent with Eq. (3.54) in the thermodynamic limit. Thus, panel (b) indicates an anomaly that shows TL phase (Ⅱ). Panel (c) appears to indicate that A becomes finite. However, when m approaches zero, the high-order differential of free energy becomes infinite from Eq. (2.26). Therefore, the A at $m = 1/N$ approaches infinity as the system size becomes larger and shows an anomaly that indicates Kosterlitz–Thouless (KT) transition. Panel (d) demonstrates that A is infinity and is consistent with Eq. (3.16) in the thermodynamic limit. Thus, panel (d) shows an anomaly that indicates a Neel state that is double degeneracy of the ground state with energy gap.

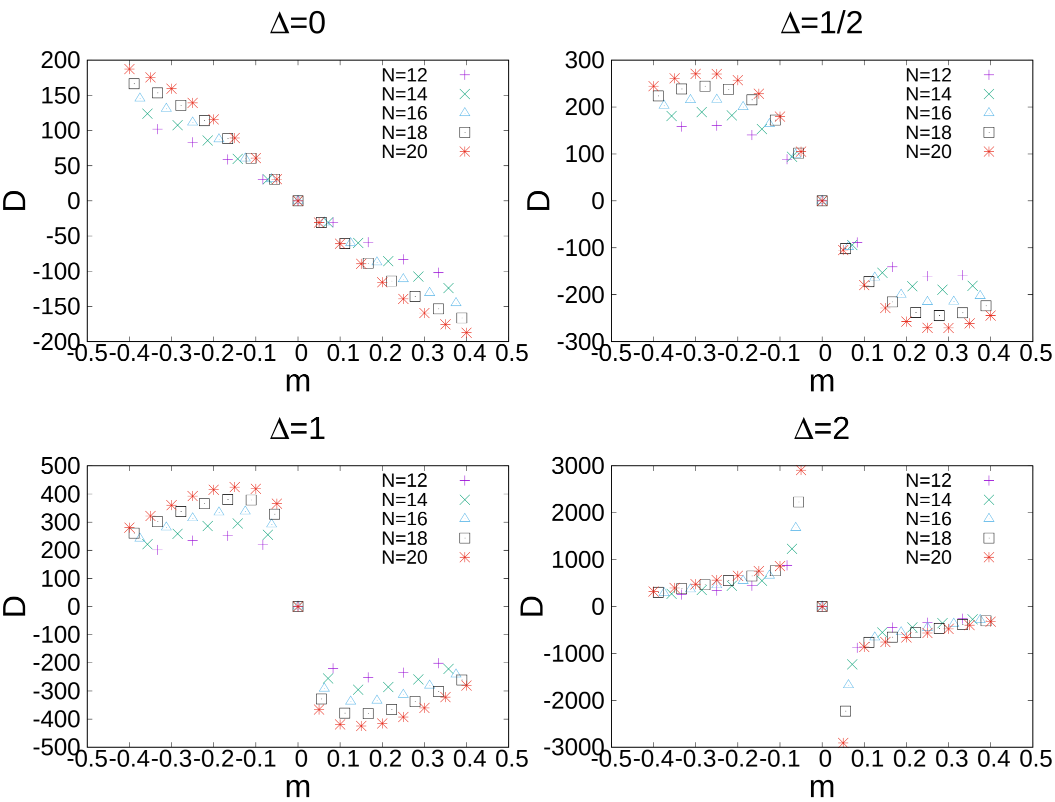

Fig. 6.5: Magnetization m dependence of the third derivative D of the $S = 1/2$ XXZ antiferromagnetic chain for several system sizes N: 12, 14, 16, 18, 20. For $\Delta = 0$ and $1/2$, D shows smooth curves. In contrast, for $\Delta = 1$ and 2, D at $m = 1/N$ shows cusps and high size dependence.

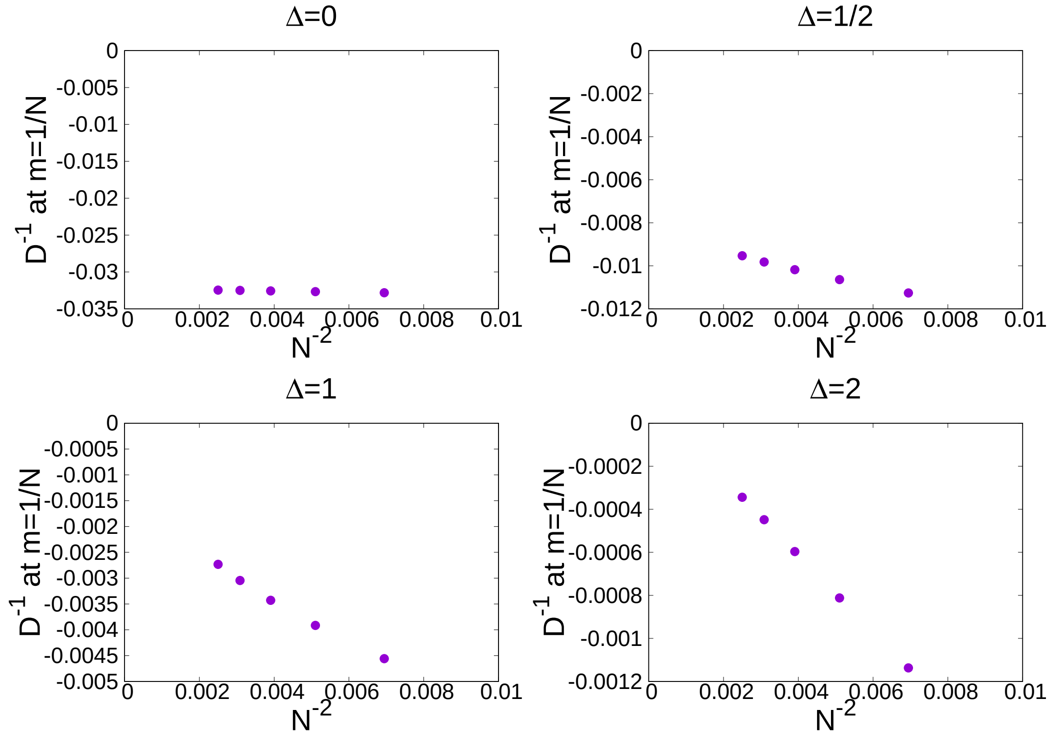

Fig. 6.6: N^{-2} dependence of the third derivative D^{-1} at $m = 1/N$. For $\Delta = 0$ and $1/2$, D becomes constant in the thermodynamic limit. In contrast, D for $\Delta = 1$ approaches minus infinity and is consistent with Eq. (2.26). Thus, for $\Delta = 1$, D shows an anomaly that indicates Kosterlitz–Thouless (KT) transition. In addition, D for $\Delta = 2$ approaches minus infinity and is consistent with Eq. (6.7). Therefore, D for $\Delta = 2$ shows an anomaly that indicates a Neel state which is double degeneracy of the ground state with energy gap.

Chapter 7

Conclusion

We investigated anomalies of magnetic susceptibility χ and fourth derivative A for the $S = 1/2$ XXZ antiferromagnetic chain by numerical diagonalization. Our numerical results indicate that χ^{-1} shows an anomaly for $\Delta > 1$ and A clearly shows an anomaly for $\Delta > 1/2$ at zero magnetization. In addition, A at magnetization $m = 1/N$ where N is the system size shows an anomaly for $\Delta > 1$. In contrast, in the $\Delta < 0$ region, the anomalies of χ and A in numerical calculations are left for future works. These results indicate that χ and A have anomalies, and that observing the anomaly of A is easier than that of χ for relatively small system sizes. Moreover, we reveal that the Tomonaga–Luttinger (TL) phase can be divided into $-1 < \Delta < 1/2$ as TL phase (I) and $1/2 < \Delta \leq 1$ as TL phase (I I), from the perspective of the anomaly of A at $\Delta = 1/2$. Therefore, we conclude that observation of A is a useful method for analyzing critical phenomena, compared with that of χ. The anomalies of third derivative D is shown for $\Delta \geq 1$ at $m = 1/N$. However, the theory related to D is left for future works.

The behavior of spin liquids has been studied for magnetic susceptibility. Our method using A, compared with that using χ, will be appropriate for researching the behavior of a spin liquid that has spin gap issues. In addition, observation of A will be useful for investigating $N = 2$ SUSY. However, our studies do not include the case of open boundary conditions or other boundary conditions. This should be resolved in our future studies. Our study is concerned with one-dimensional systems. However, our method can be used regardless of dimensions. This method will help investigate quantum spin systems in two or three dimensions. The observation of A has an important role in experiments, as A relates to the nonlinear magnetic susceptibility which shows the behavior of spin–glass in quantum spin systems. The nonlinear magnetic susceptibility can be easily calculated by using χ, A, and D.

The method using A can be a new technique in the study of quantum spin systems and strongly correlated electron systems. Numerical diagonalization calculations of A will provide a new development in theory and experiments for quantum spin systems.

Acknowledgment

I would like to acknowledge the help and support which I have received from many people throughout my Ph.D studies.

First of all, I would like to thank my supervisor Professor Kiyohide Nomura for leading the way to scientific research, always having time for discussions, giving the advice on numerical calculations, having my manuscript read, and above all his continuous encouragement. I have learned theoretical methods used in this thesis from him. Without him, I could not have completed this work.

I would like to thank Professor Hosho Katsura for giving useful comments and rigorous discussions. I would like to express my sincere gratitude for his clear suggestions for the further development of this research. He taught me the studies of quantum spin systems, especially Bethe ansatz.

I would like to thank Professor Jun-ichi Fukuda for giving useful suggestions and heart-warming encouragement and having my manuscript read. He gave me a lot of knowledge concerning writing manuscript and English expressions.

I would like to thank all of our research group members, especially Professor Hiizu Nakanishi and Professor Jun Matsui for helping my study. I also would like to thank Professor Toru Sakai, Professor Minoru Takahashi, and Professor Chihiro Matsui for the helpful discussions on my study.

Our calculations on numerical diagonalization were performed using TIT-PACK Ver.2, which Professor Hidetoshi Nishimori coded, and $H\phi$, which Professor Mitsuaki Kawamura *et al.* coded.

Finally, I would like to thank my parents for their warm support, encouragement, and patience for years.

Appendix A

Calculation method

Lanczos method is calculation method using diagonalization and improvement of iterative method. Iterative method is method to calculate eigenvalue to matrix H by multiplying repeatedly H by initial vector v_0. In other words, when n dimension matrix H has eigenvalue, eigenvector $E_j, \psi_j (j = 1 - n)$, the initial vector v_0 is expanded in the following way

$$v_0 = \sum_{i=j}^{n} a_j \psi_j, \tag{A.1}$$

where a_j is a coefficient. Multiplying H^k by Eq. (A.1), we obtain

$$v_k = H^k v_0 = \sum_{i=j}^{n} a_j (E_j)^k \psi_j. \tag{A.2}$$

When k increases, weight of eigenstate increases. In Lanczos method, we give triple diagonalization matrix T that $T = V^{-1}HV$. The orthogonal column vector to H is defined as $V = (v_1, v_2, ...)$. T is written in the form

$$T = \begin{pmatrix} \alpha_1 & \beta_1 & \dots & \dots & 0 \\ \beta_1 & \alpha_2 & \ddots & 0 & \vdots \\ \vdots & \ddots & \ddots & \ddots & \vdots \\ \vdots & 0 & \ddots & \ddots & \beta_n \\ 0 & \dots & \dots & \beta_n & \alpha_n \end{pmatrix}, \tag{A.3}$$

where α_i and β_i are nonzero constants. T is called as tridiagonal matrix. Considering $TV = HV$, the relation is

$$\begin{aligned}
Hv_1 &= \alpha_1 v_1 + \beta_1 v_2, \\
Hv_2 &= \beta_1 v_1 + \alpha_2 v_2 + \beta_2 v_3, \\
&\vdots \\
Hv_k &= \beta_{k-1} v_{k-1} + \alpha_k v_k + \beta_k v_{k+1}, \\
&\vdots \\
Hv_m &= \beta_{m-1} v_{m-1} + \alpha_m v_m.
\end{aligned} \tag{A.4}$$

When we multiply v_k by kth component in Eq. (A.4), α is given by

$$\alpha_k = v_k^{\mathrm{T}} H v_k. \tag{A.5}$$

The kth component in Eq. (A.4) is transformed in the form

$$u_{k+1} = Hv_k - \beta_{k-1} v_{k-1} - \alpha_k v_k, \tag{A.6}$$

where $u_{k+1} = \beta_k v_{k+1}$. To satisfy $v_{k+1}^{\mathrm{T}} v_{k+1} = 1$, β_k is defined as

$$\beta_k = ||Hv_k - \beta_{k-1} v_{k-1} - \alpha_k v_k||. \tag{A.7}$$

Thus, Lanczos method is simplified by calculation of α_k and β_k.

Appendix B

Gaussian model and Sine-Gordon model

In this chapter, we review Nomura's work [18], which shows the symmetry of the gaussian model and sine-Gordon model. In addition, we indicate that XXZ chain is equivalent to the sine-Gordon model in detail.

B.1 Gaussian model

We introduce Lagrangian $\mathcal{L}$ of the 2D gaussian model defined as

$$\mathcal{L} = \frac{1}{2\pi K}(\nabla\phi)^2, \tag{B.1}$$

where ϕ is a complex field and K is a parameter. To derive the two-point correlation function, the multivariable gaussian integration is needed as following

$$\int d\boldsymbol{x} \exp\left[-\frac{1}{2}{}^t\boldsymbol{x}A\boldsymbol{x}\right] = (2\pi)^{\frac{N}{2}}(\det A)^{-\frac{1}{2}}, \tag{B.2}$$

where A is $N \times N$ real symmetric matrix and $\boldsymbol{x}$ is N real vector. The two-point correlation function is given in the form

$$\langle x_q x_r \rangle = A^{-1}_{rq} \equiv G_{rq}, \tag{B.3}$$

where G_{rq} is a green function. Subsequently, Eq. (B.3) is rewritten in the form

$$\sum_j A_{ij}G_{jk} = \delta_{ik}, \tag{B.4}$$

where G is regarded as green function to A. In the conformal field theory of 2D gaussian model, the relation such as Eq. (B.4) is written as

$$\frac{1}{\pi K}\partial_{r_1}\partial_{r_2}\langle\phi(z_1,\overline{z}_1)\phi(z_2,\overline{z}_2)\rangle = \delta(z_1-z_2)$$
$$\frac{4}{\pi K}\partial_{z_1}\partial_{\overline{z}_2}\langle\phi(z_1,\overline{z}_1)\phi(z_2,\overline{z}_2)\rangle = \delta(z_1-z_2), \tag{B.5}$$

where the two independent complex coordinates $z \equiv x+iy, \overline{z} \equiv x-iy$ and

$$\partial_z = \frac{1}{2}\left(\frac{\partial}{\partial x} - i\frac{\partial}{\partial y}\right), \tag{B.6}$$

$$\partial_{\overline{z}} = \frac{1}{2}\left(\frac{\partial}{\partial x} + i\frac{\partial}{\partial y}\right), \tag{B.7}$$

$$\partial_r^2 = \partial_x^2 + \partial_y^2. = 4\partial_z\partial_{\overline{z}}. \tag{B.8}$$

We then utilize the formula of two dimensional Green function:

$$\Delta \ln|z-w|^2 \equiv 4\partial_z\partial_{\overline{z}}\ln|z-w|^2 = -2\pi\delta(z-w), \tag{B.9}$$

where w is complex and a holomorphic function. When Eq. (B.5) is compared with Eq. (B.9), the two-point correlation function of ϕ is given

$$\frac{1}{\pi K}\langle\phi(z_1,\overline{z}_1)\phi(z_2,\overline{z}_2)\rangle = -\frac{1}{2\pi}\ln\left|\frac{z_1-z_2}{\alpha}\right|^2$$
$$\langle\phi(z_1,\overline{z}_1)\phi(z_2,\overline{z}_2)\rangle = -\frac{K}{2}\ln\left|\frac{z_{12}}{\alpha}\right|^2, \tag{B.10}$$

where $z_{12} = z_1 - z_2$ and α is cut-off. The function $\phi(z,\overline{z})$ could be divided into holomorphic and non-holomorphic part.

$$\phi(z,\overline{z}) = \phi(z) + \phi(\overline{z}). \tag{B.11}$$

Subsequently, the two-point correlation functions of $\phi(z)$ and $\phi(\overline{z})$ are given by

$$\langle\phi(z_1)\phi(z_2)\rangle = -\frac{K}{2}\ln\left|\frac{z_{12}}{\alpha}\right|, \langle\phi(\overline{z}_1)\phi(\overline{z}_2)\rangle = -\frac{K}{2}\ln\left|\frac{\overline{z_{12}}}{\alpha}\right|. \tag{B.12}$$

As an expansion of the above equations, we consider the two-point correlation functions of the exponential operator to ϕ as follows

$$\begin{aligned}\langle\exp(ie\phi(z_1))\exp(-ie\phi(z_2))\rangle &= \left\langle\sum_{n=1}^{\infty}\frac{1}{n!}(ie\phi)^n\sum_{m=1}^{\infty}\frac{1}{m!}(-ie\phi)^m\right\rangle \\ &= \sum_{n,m=1}^{\infty}\frac{1}{n!m!}(ie)^{n+m}(-1)^m\langle\phi(z_1)^n\phi(z_2)^m\rangle,\end{aligned} \tag{B.13}$$

where e is a charge. When $z_1 \neq z_2$, from Wick's theorem Eq. (B.13) is transformed as

$$\begin{aligned}\langle \exp\left(ie\phi(z_1)\right)\exp\left(-ie\phi(z_2)\right)\rangle &= \sum_{n=1}^{\infty}\frac{1}{n!}\left(e^2\langle\phi(z_1)\phi(z_2)\rangle\right)^n \\ &= \exp\left(e^2\langle\phi(z_1)\phi(z_2)\rangle\right) \\ &= \left|\frac{z_{12}}{\alpha}\right|^{\frac{Ke^2}{2}}. \end{aligned}\tag{B.14}$$

Next, we consider the symmetry of the gaussian model (B.1). Under $\phi \to \phi' = \phi + a$ where a is a constant and $\phi \to \phi' = -\phi$, Eq. (B.1) is invariant. The translational and inversion symmetry compactify the field ϕ in a circle. Subsequently, in order to consider the symmetry of the gaussian model and sine-Gordon model introducing in next section, we give a new field $\theta(z,\overline{z})$. The $\theta(z,\overline{z})$ is defined as

$$\theta(z,\overline{z}) = \theta(z) + \theta(\overline{z}) = \frac{1}{K}\left[\phi(z) - \phi(\overline{z})\right], \tag{B.15}$$

where $\theta(z), \theta(\overline{z})$ are holomorphic and non-holomorphic part of $\theta(z,\overline{z})$. The θ is called as a dual field to ϕ. And then, the relation between ϕ and θ is defined as

$$(\partial_x - \partial_{\overline{z}})\phi = (\partial_z + \partial_{\overline{z}})K\theta. \tag{B.16}$$

Using Eq. (B.12), the the two-point correlation function related to θ is given by

$$\langle\theta(z_1)\theta(z_2)\rangle = -\frac{1}{2K}\,\mathrm{Re}\ln\left|\frac{z_{12}}{\alpha}\right|, \tag{B.17}$$

$$\langle\phi(z_1)\theta(z_2)\rangle = -i\,\mathrm{Im}\ln\left|\frac{z_{12}}{\alpha}\right|. \tag{B.18}$$

In $\phi \to \phi' = \phi + a$ where a is a constant and $\theta \to \theta' = \theta + a$, Eq. (B.16) is invariant. This means the rotational invariance in a circle. Thus, the gaussian model (B.1) has $U(1) \times U(1)$ symmetry. In addition, these indicate that the symmetry of the gaussian model compactify ϕ and θ in a two circle, that is, ϕ and θ are mapped in a two dimensional cylinder.

Finally, we consider the scaling dimension when the dual field θ is introduced. The scaling dimension is closely related to the two-point correlation function as the exponent of the correlation function is equivalent to the scaling dimension [39]. In general, the two-point correlation function of the gaussian model is given by

$$\begin{aligned}&\langle O_{n,m}(z_1)\,O_{-n,-m}(z_2)\rangle \\ &= \exp\left[-\left(n^2K + \frac{m^2}{K}\right)\mathrm{Re}\log\left(\frac{z_{12}}{\alpha}\right) - 2inm\left(\mathrm{Arg}\left(\frac{z_{12}}{\alpha}\right) + \frac{\pi}{2}\right)\right],\end{aligned}\tag{B.19}$$

$$O_{n,m} \equiv \exp(in\sqrt{2}\phi)\exp(im\sqrt{2}\theta), \tag{B.20}$$

where m is a magnetization and $\mathrm{Arg}(z_{12}) = \mathrm{Im}\ln z_{12}$ is an angle between $\vec{z_1}$ and $\vec{z_2}$. We then prove Eq. (B.19). With reference to Eq. (B.14), $\langle O_{n,m}O_{-n,-m}\rangle$ is

$$\begin{aligned}
&\langle O_{n,m}O_{-n,-m}\rangle \\
&= \sum_{\alpha=1}^{\infty} \frac{1}{\alpha!} \left[n^2 \langle\phi(z_1)\phi(z_2)\rangle + m^2 \langle\theta(z_1)\theta(z_2)\rangle + nm \langle\phi(z_1)\theta(z_2)\rangle\right. \\
&\left.+nm \langle\theta(z_1)\phi(z_2)\rangle\right]^\alpha \\
&= \exp\left(n^2 \langle\phi(z_1)\phi(z_2)\rangle + m^2 \langle\theta(z_1)\theta(z_2)\rangle + nm \langle\phi(z_1)\theta(z_2)\rangle\right. \\
&\left.+nm \langle\theta(z_1)\phi(z_2)\rangle\right) \\
&= \exp\left[-n^2 K \,\mathrm{Re}\ln\frac{z_{12}}{\alpha}\right] \exp\left[-\frac{m^2}{K}\mathrm{Re}\ln\frac{z_{12}}{\alpha}\right] \exp\left[-inm\,\mathrm{Im}\ln\frac{z_{12}}{\alpha}\right] \\
&\times \exp\left[-inm\,\mathrm{Im}\ln\frac{z_{21}}{\alpha}\right] \\
&= \exp\left[-\left(n^2K + \frac{m^2}{K}\right)\mathrm{Re}\log\left(\frac{z_{12}}{\alpha}\right) - 2inm\left(\mathrm{Arg}\left(\frac{z_{12}}{\alpha}\right) + \frac{\pi}{2}\right)\right], \qquad \text{(B.21)}
\end{aligned}$$

where

$$\begin{aligned}
-inm\,\mathrm{Im}\ln\frac{z_{21}}{\alpha} &= -inm\,\mathrm{Im}\left[\ln\frac{z_{12}}{\alpha} + \ln(-1)\right] \\
&= -inm\,\mathrm{Im}\left[\ln\frac{z_{12}}{\alpha} + \ln e^{i\pi}\right] \\
&= -inm\,\mathrm{Im}\left[\ln\frac{z_{12}}{\alpha} + i\pi\right] \\
&= -inm\left(\mathrm{Im}\ln\frac{z_{12}}{\alpha} + \pi\right).
\end{aligned}$$

Therefore, Eq. (B.19) is proved. Here, the scaling dimension $x_{n,m}$ and spin $l_{n,m}$ are defined as

$$x_{n,m} = \frac{1}{2}\left(n^2K + \frac{m^2}{K}\right), \qquad \text{(B.22)}$$

$$l_{n,m} = nm. \qquad \text{(B.23)}$$

The scaling dimension is derived from Eq. (B.19) in the following way

$$\exp\left[-\left(n^2K + \frac{m^2}{K}\right)\ln\left(\frac{z_{12}}{\alpha}\right) + ...\right] = C_1\left|\frac{z_{12}}{\alpha}\right|^{-\left(n^2K+\frac{m^2}{K}\right)}, \qquad \text{(B.24)}$$

where C_1 is a constant and n, m are corresponded to a charge and magnetization. The exponent $-(n^2K + \frac{m^2}{K})$ is equivalent to $-2x_{n,m}$. The model is changed when n, m varies. For example, when $(n, m) = (2, 0)$, the scaling dimension of the gaussian model is equivalent to that of $S = 1/2$ XXZ chain.

B.2 Sine-Gordon model

We introduce the sine-Gordon model corresponding to XXZ chain that has $U(1)$ symmetry. The sine-Gordon model is defined as

$$\mathcal{L} = \frac{1}{2\pi K}(\nabla\phi)^2 + \frac{y_\phi}{2\pi\alpha^2}\cos\sqrt{8}\phi. \tag{B.25}$$

We then compactify the field ϕ in a circle such as the gaussian model. In $\phi \to \phi' = \phi + 2\pi/\sqrt{8}$, the transformation of Lagrangian is written in the form

$$\begin{aligned}\mathcal{L} \to \mathcal{L}' &= \frac{1}{2\pi K}(\nabla(\phi + 2\pi/\sqrt{8}))^2 + \frac{y_\phi}{2\pi\alpha^2}\cos(\sqrt{8}\phi + 2\pi) \\ &= \frac{1}{2\pi K}(\nabla\phi)^2 + \frac{y_\phi}{2\pi\alpha^2}\cos\sqrt{8}\phi = \mathcal{L}.\end{aligned}$$

From the above equation, Lagrangian is invariant. Under $\phi \to \phi' = \phi + 2\pi/\sqrt{8}$, the model (B.25) shows Z_2 symmetry that means the spin reversal. As the sine-Gordon model is corresponded to XXZ chain that has $U(1)$ symmetry, the model needs to be $U(1)$ symmetry. Subsequently, we introduce the deal field θ. In $\theta \to \theta + 2\pi/\sqrt{2}$, the model (B.25) shows $U(1)$ symmetry. The term $\cos\sqrt{8}\phi$ in Eq. (B.25) means an irrelevant field. Considering the renormalization which shows the behavior of critical phenomena, when the irrelevant field is ignored, critical phenomena of the sine-Gordon model is equal to the gaussian model. Thus, for the sine-Gordon model, scaling dimension is equivalent to Eq. (B.22).

B.3 Sine-Gordon model and XXZ chain

We introduce the explicit correspondence between XXZ chain and the sine-Gordon model. First, we define $S = 1/2$ antiferromagnetic XXZ chain in the form

$$\hat{\mathscr{H}} = J\sum_{j=1}^{N}(\hat{S}_j^x\hat{S}_{j+1}^x + \hat{S}_j^y\hat{S}_{j+1}^y + \Delta\hat{S}_j^z\hat{S}_{j+1}^z), \tag{B.26}$$

where $\hat{S}_j^x, \hat{S}_j^y, \hat{S}_j^z$ is the spin operator on jth site in the x, y, z direction, J is an exchange interaction, and N is the system size. We then rewrite the chain to fermion system by using Jordan-Wigner transformation. Jordan-Wigner transformation is defined as

$$\hat{S}_j^+ = \hat{S}_j^x + i\hat{S}_j^y = \hat{a}_j^\dagger e^{i\pi\sum_{l<j}\hat{a}_l^\dagger\hat{a}_l}, \tag{B.27}$$

$$\hat{S}_j^- = \hat{S}_j^x - i\hat{S}_j^y = \hat{a}_j e^{-i\pi\sum_{l<j}\hat{a}_l^\dagger\hat{a}_l}, \tag{B.28}$$

$$\hat{S}_j^z = \hat{a}_j^\dagger\hat{a}_j - \frac{1}{2}, \tag{B.29}$$

where $\hat{a}_j^\dagger, \hat{a}_j$ are fermion creation and annihilation operator on the jth site. The anticommutation relation is given by

$$\{\hat{a}_j, \hat{a}_k^\dagger\} = \delta_{jk}, \{\hat{a}_j^\dagger, \hat{a}_k^\dagger\} = \{\hat{a}_j, \hat{a}_k\} = 0. \tag{B.30}$$

Using Jordan-Wigner transformation, the spin $\hat{S}_j^+ \hat{S}_{j+1}^-$ is written as follows

$$\begin{aligned}\hat{S}_j^+ \hat{S}_{j+1}^- &= \hat{a}_j^\dagger e^{i\pi \sum_{l<j} \hat{a}_l^\dagger \hat{a}_l} \hat{a}_{j+1} e^{i\pi \sum_{l<j+1} \hat{a}_l^\dagger \hat{a}_l} \\ &= \hat{a}_j^\dagger \hat{a}_{j+1} e^{i\pi \hat{a}_j^\dagger \hat{a}_j} = \hat{a}_j^\dagger \hat{a}_{j+1}.\end{aligned}$$

Thus, Hamiltonian of the chain (B.26) is rewrote by

$$\hat{\mathscr{H}} = J \sum_{j=1}^{N} \left[\frac{1}{2} \left(\hat{a}_j^\dagger \hat{a}_{j+1} + \hat{a}_{j+1}^\dagger \hat{a}_j \right) + \Delta \left(\hat{a}_j^\dagger \hat{a}_j - \frac{1}{2} \right) \left(\hat{a}_{j+1}^\dagger \hat{a}_{j+1} - \frac{1}{2} \right) \right]. \tag{B.31}$$

The x, y component of the chain is regarded as hopping term of fermion. The z component of the chain gives interaction between fermions. The XXZ chain is equivalent to fermion system with interaction.

Next, we carry out bosonization of XXZ chain for $|\Delta| \ll 1$. The bosonization means the transformation from fermion field to boson field for taking continuous limit in lattice model. For XX chain that means the XXZ chain of $\Delta = 0$, the fermion operator $\hat{a}_j$ is

$$\hat{a}_j = \sqrt{a} \left(e^{-\frac{i\pi x}{2a}} \hat{\psi}_R(x) + e^{\frac{i\pi x}{2a}} \hat{\psi}_L(x) \right), \tag{B.32}$$

where a is lattice spacing, $x = ja$, and $\hat{\psi}_R, \hat{\psi}_L$ are a right and left mover of fermion field operator in the form

$$\hat{\psi} = e^{ik_F x} \hat{\psi}_R(x) + e^{-ik_F x} \hat{\psi}_L(x),$$

where $\hat{\psi}$ is fermion field operator and k_F is Fermi wavenumber. Subsequently, the

x, y component in Eq. (B.26), that is, $\hat{\mathscr{H}}_{XX}$ is defined as

$$
\begin{aligned}
&\hat{\mathscr{H}}_{XX} \\
&= \frac{Ja}{2}\sum_{j=1}^{N}\Big[(e^{\frac{i\pi x}{2a}}\hat{\psi}_R^\dagger(x) + e^{\frac{-i\pi x}{2a}}\hat{\psi}_L^\dagger(x))(e^{\frac{-i\pi(x+a)}{2a}}\hat{\psi}_R(x+a) + e^{\frac{i\pi(x+a)}{2a}}\hat{\psi}_L(x+a)) \\
&+(e^{\frac{i\pi(x+a)}{2a}}\hat{\psi}_R^\dagger(x+a) + e^{\frac{-i\pi(x+a)}{2a}}\hat{\psi}_L^\dagger(x+a))(e^{\frac{-i\pi x}{2a}}\hat{\psi}_R(x) + e^{\frac{i\pi x}{2a}}\hat{\psi}_L(x))\Big] \\
&\simeq \frac{iJa}{2}\sum_{j=1}^{N}\Big[-\hat{\psi}_R^\dagger(x)\hat{\psi}_R(x+a) + \hat{\psi}_L^\dagger(x)\hat{\psi}_L(x+a) + \hat{\psi}_R^\dagger(x+a)\hat{\psi}_R(x) \\
&-\hat{\psi}_L^\dagger(x+a)\hat{\psi}_L(x)\Big] \\
&= \frac{iJa}{2}\int dx\left[\hat{\psi}_L^\dagger(x)\frac{\mathrm{d}\hat{\psi}_L(x)}{\mathrm{d}x} - \frac{\mathrm{d}\hat{\psi}_L^\dagger(x)}{\mathrm{d}x}\hat{\psi}_L(x) - \hat{\psi}_R^\dagger(x)\frac{\mathrm{d}\hat{\psi}_R(x)}{\mathrm{d}x} + \frac{\mathrm{d}\hat{\psi}_R^\dagger(x)}{\mathrm{d}x}\hat{\psi}_R(x)\right] \\
&= \frac{iJa}{2}\int dx 2\left[\hat{\psi}_L^\dagger(x)\frac{\mathrm{d}\hat{\psi}_L(x)}{\mathrm{d}x} - \hat{\psi}_R^\dagger(x)\frac{\mathrm{d}\hat{\psi}_R(x)}{\mathrm{d}x}\right], \qquad \text{(B.33)}
\end{aligned}
$$

where we ignore oscillation term $e^{\pm\frac{i\pi x}{a}}$ and $\hat{\psi}(x+a) - \hat{\psi}(x) = a\frac{\mathrm{d}\hat{\psi}(x)}{\mathrm{d}x}$ for continuous limit $a\sum_j \to \int dx$. The correspondence between fermion fields $\hat{\psi}_L$ and boson fields is written as

$$
\begin{aligned}
i\hat{\psi}_L^\dagger(x)\frac{\mathrm{d}\hat{\psi}_L(x)}{\mathrm{d}x} &\leftrightarrow \frac{1}{4\pi}\left(\frac{\mathrm{d}\hat{\varphi}_L(x)}{\mathrm{d}x}\right)^2 = \frac{1}{4}\left(\frac{\mathrm{d}\hat{\phi}(x)}{\mathrm{d}x} + \frac{\mathrm{d}\hat{\theta}(x)}{\mathrm{d}x}\right)^2, \\
-i\hat{\psi}_R^\dagger(x)\frac{\mathrm{d}\hat{\psi}_R(x)}{\mathrm{d}x} &\leftrightarrow \frac{1}{4\pi}\left(\frac{\mathrm{d}\hat{\varphi}_R(x)}{\mathrm{d}x}\right)^2 = \frac{1}{4}\left(\frac{\mathrm{d}\hat{\phi}(x)}{\mathrm{d}x} - \frac{\mathrm{d}\hat{\theta}(x)}{\mathrm{d}x}\right)^2.
\end{aligned}
$$

where $\hat{\varphi}_L, \hat{\varphi}_R$ are boson field operators and two boson field operators $\hat{\phi}(x), \hat{\theta}(x)$ are defined as

$$\hat{\phi}(x) = \frac{1}{\sqrt{4\pi}}\left[\hat{\varphi}_L(x) + \hat{\varphi}_R(x)\right], \qquad \text{(B.34)}$$

$$\hat{\theta}(x) = \frac{1}{\sqrt{4\pi}}\left[\hat{\varphi}_L(x) - \hat{\varphi}_R(x)\right], \qquad \text{(B.35)}$$

$$\hat{\Pi}(x) = \frac{\mathrm{d}\hat{\theta}(x)}{\mathrm{d}x}. \qquad \text{(B.36)}$$

where $[\hat{\phi}(x), \hat{\Pi}(y)] = i\delta(x-y)$ and $\hat{\Pi}$ is conjugate operator to $\hat{\phi}$. And then, Eq. (B.33) is written in the form

$$\hat{\mathscr{H}}_{XX} = Ja\int dx\frac{1}{4\pi}\left[\left(\frac{\mathrm{d}\hat{\varphi}_L(x)}{\mathrm{d}x}\right)^2+\left(\frac{\mathrm{d}\hat{\varphi}_R(x)}{\mathrm{d}x}\right)^2\right]$$
$$= \frac{Ja}{4}\int dx 2\left[\left(\frac{\mathrm{d}\hat{\phi}(x)}{\mathrm{d}x}\right)^2+\left(\frac{\mathrm{d}\hat{\theta}(x)}{\mathrm{d}x}\right)^2\right]$$
$$= \frac{Ja}{2}\int dx\left[\left(\frac{\mathrm{d}\hat{\phi}(x)}{\mathrm{d}x}\right)^2+\hat{\Pi}^2(x)\right]. \qquad \text{(B.37)}$$

Next, we consider the bosonization of $\hat{S}^z_j$. Using Eq. (B.32), $\hat{S}^z_j$ is written in the form

$$\hat{S}^z_j = a\left(e^{\frac{i\pi x}{2a}}\hat{\psi}^\dagger_R(x)+e^{-\frac{i\pi x}{2a}}\hat{\psi}^\dagger_L(x)\right)\left(e^{-\frac{i\pi x}{2a}}\hat{\psi}_R(x)+e^{\frac{i\pi x}{2a}}\hat{\psi}_L(x)\right)-1/2$$
$$= a\left[\hat{\psi}^\dagger_R(x)\hat{\psi}_R(x)+\hat{\psi}^\dagger_L(x)\hat{\psi}_L(x)+e^{\frac{i\pi x}{a}}\hat{\psi}^\dagger_R(x)\hat{\psi}_L(x)\right.$$
$$\left.+e^{-\frac{i\pi x}{a}}\hat{\psi}^\dagger_L(x)\hat{\psi}_R(x)\right]-1/2$$
$$= a(:\hat{\psi}^\dagger_R(x)\hat{\psi}_R(x):+:\hat{\psi}^\dagger_L(x)\hat{\psi}_L(x):)+a(-1)^{x/a}(\hat{\psi}^\dagger_R(x)\hat{\psi}_L(x)$$
$$+\hat{\psi}^\dagger_L(x)\hat{\psi}_R(x)), \qquad \text{(B.38)}$$

where $e^{i\pi x/a} = (-1)^{x/a}$, the sign ': :' is normal order product, and $\langle\hat{a}^\dagger_j\hat{a}_j\rangle = \langle\hat{\psi}^\dagger_R(x)\hat{\psi}_R\rangle+\langle\hat{\psi}^\dagger_L(x)\hat{\psi}_L\rangle = 1/2$. When $\hat{\psi}_L, \hat{\psi}_R$ are independent, the fermion fields and the boson field are related as follows

$$\hat{\psi}_L(x) \leftrightarrow \frac{e^{-i\hat{\varphi}_L(x)}}{\sqrt{2\pi\alpha}}, \qquad \text{(B.39)}$$
$$\hat{\psi}_R(x) \leftrightarrow \frac{e^{i\hat{\varphi}_R(x)}}{\sqrt{2\pi\alpha}}, \qquad \text{(B.40)}$$
$$:\hat{\psi}^\dagger_L(x)\hat{\psi}_L(x): \leftrightarrow \frac{1}{2\pi}\frac{\mathrm{d}\hat{\varphi}_L}{\mathrm{d}x}, \qquad \text{(B.41)}$$
$$:\hat{\psi}^\dagger_R(x)\hat{\psi}_R(x): \leftrightarrow \frac{1}{2\pi}\frac{\mathrm{d}\hat{\varphi}_R}{\mathrm{d}x}, \qquad \text{(B.42)}$$
$$\text{(B.43)}$$

where α is cut-off. From the above equations, Eq. (B.38) is given by

$$\hat{S}^z_j = \frac{a}{2\pi}\left(\frac{\mathrm{d}\hat{\varphi}_L}{\mathrm{d}x}+\frac{\mathrm{d}\hat{\varphi}_R}{\mathrm{d}x}\right)+\frac{a(-1)^{x/a}}{2\pi\alpha}\left[e^{-i\hat{\varphi}_R}e^{-i\hat{\varphi}_L}+e^{i\hat{\varphi}_L}e^{i\hat{\varphi}_R}\right]$$
$$= \frac{a}{\sqrt{\pi}}\frac{\mathrm{d}\hat{\phi}}{\mathrm{d}x}+\frac{a(-1)^{x/a}}{2\pi\alpha}2\cos[\sqrt{4\pi}\hat{\phi}(x)]. \qquad \text{(B.44)}$$

Hamiltonian in z component of XXZ chain $\hat{\mathscr{H}}_z = \Delta J \sum_j \hat{S}_j^z \hat{S}_{j+1}^z$ is described:

$$\begin{aligned}
\hat{\mathscr{H}}_z &= a^2 \Delta J \sum_j \left(\frac{1}{\sqrt{\pi}} \frac{\mathrm{d}\hat{\phi}(x)}{\mathrm{d}x} + \frac{(-1)^{x/a}}{\pi\alpha} \cos\left[\sqrt{4\pi}\hat{\phi}(x)\right] \right) \\
&\times \left(\frac{1}{\sqrt{\pi}} \frac{\mathrm{d}\hat{\phi}(x+a)}{\mathrm{d}x} + \frac{(-1)^{x/a}}{\pi\alpha} \cos\left[\sqrt{4\pi}\hat{\phi}(x+a)\right] \right) \\
&\simeq a\Delta J \int dx \left(\frac{1}{\pi} \frac{\mathrm{d}\hat{\phi}(x)}{\mathrm{d}x} \frac{\mathrm{d}\hat{\phi}(x+a)}{\mathrm{d}x} - \frac{1}{\pi^2\alpha^2} \cos\left[\sqrt{4\pi}\hat{\phi}(x)\right] \cos\left[\sqrt{4\pi}\hat{\phi}(x+a)\right] \right),
\end{aligned} \tag{B.45}$$

where we ignore oscillation terms $(-1)^{x/a}$. In $x \gg a$, $\frac{\mathrm{d}\hat{\phi}(x+a)}{\mathrm{d}x} \simeq \frac{\mathrm{d}\hat{\phi}(x)}{\mathrm{d}x}$. Thus, $\hat{\mathscr{H}}_z$ is given as follows

$$\begin{aligned}
\hat{\mathscr{H}}_z &= a\Delta J \int dx \left[\frac{1}{\pi} \left(\frac{\mathrm{d}\hat{\phi}(x)}{\mathrm{d}x} \right)^2 - \frac{1}{2\pi^2\alpha^2} \cos\sqrt{4\pi}[\hat{\phi}(x+a) + \hat{\phi}(x)] \right. \\
&\left. - \frac{1}{2\pi^2\alpha^2} \cos\sqrt{4\pi}[\hat{\phi}(x+a) - \hat{\phi}(x)] \right] \\
&\simeq a\Delta J \int dx \left[\frac{1}{\pi} \left(\frac{\mathrm{d}\hat{\phi}(x)}{\mathrm{d}x} \right)^2 - \frac{1}{2\pi^2\alpha^2} \cos\left(\sqrt{16\pi}\hat{\phi}(x)\right) \right].
\end{aligned} \tag{B.46}$$

For $a \to 0$, $\hat{\phi}(x+a) + \hat{\phi}(x) \simeq 2\hat{\phi}(x)$ and we ignore the constant term. Using Eq. (B.37) and Eq. (B.46), Hamiltonian of XXZ chain is represented as

$$\begin{aligned}
\hat{\mathscr{H}} &= \frac{aJ}{2} \int dx \left[\left(1 + \frac{2\Delta}{\pi}\right) \left(\frac{\mathrm{d}\hat{\phi}}{\mathrm{d}x} \right)^2 + \hat{\Pi}^2 - \frac{\Delta}{\pi^2\alpha^2} \cos(\sqrt{16\pi}\hat{\phi}) \right] \\
&= \frac{1}{2} \int dx \left[aJ \left(\sqrt{1 + \frac{2\Delta}{\pi}} \right)^2 \left(\frac{\mathrm{d}\hat{\phi}}{\mathrm{d}x} \right)^2 + aJ\hat{\Pi}^2 - \frac{aJ\Delta}{\pi^2\alpha^2} \cos(\sqrt{16\pi}\hat{\phi}) \right] \\
&= \frac{v}{2} \int dx \left[\frac{1}{K} \left(\frac{\mathrm{d}\hat{\phi}}{\mathrm{d}x} \right)^2 + K\hat{\Pi}^2 - \frac{K\Delta}{\pi^2\alpha^2} \cos\left(\sqrt{16\pi}\hat{\phi}\right) \right],
\end{aligned} \tag{B.47}$$

where $v = aJ\sqrt{1 + 2\Delta/\pi}$ and $K = 1/\sqrt{1 + 2\Delta/\pi}$. The form of this equation is sine-Gordon model. $\frac{1}{K}\left(\frac{\mathrm{d}\hat{\phi}}{\mathrm{d}x}\right)^2 + K\hat{\Pi}^2$ corresponds to the first term of Eq. (B.25) and $-\frac{K\Delta}{\pi^2\alpha^2}\cos\left(\sqrt{16\pi}\hat{\phi}\right)$ corresponds to the second term of Eq. (B.25). Thus, XXZ chain is corresponded to sine-Gordon model in continuous limit.

Appendix C

Relation between magnetization and magnetic field

In this chapter, we introduce the the transformation between magnetization and magnetic field. As a test case, we treat spin-glass. Moreover, we discuss the transformation for XXZ chain and nonlinear magnetic susceptibility.

C.1 Case of spin-glass system

We review Suzuki's work [36], which shows the transformation between a magnetization and magnetic field for spin-glass. They focus on free energy f in the spin-glass systems as follows

$$f = -\lim_{n\to 0} \frac{k_B T}{nN} \ln Z^{(n)}, \tag{C.1}$$

where n is the number of spins, N is the number of particles, and $Z^{(n)}$ is the partition function:

$$Z^{(n)} = \langle Z^n \rangle \left\langle \mathrm{Tr} \exp\left(-\beta \sum_{k=1}^{n} \hat{H}^{(k)} \right) \right\rangle, \tag{C.2}$$

where $\hat{H}^{(k)}$ is Hamiltonian of spin-glass. For simplicity of calculation, they use replica method that is reducing $\langle \ln Z \rangle$ to Z^n where Z is a partition function and $\ln Z = \lim_{n\to 0} \frac{Z^n - 1}{n}$. Subsequently, the average $\langle ... \rangle$ denotes the average over random distribution of exchange interaction $P(\{J\})$:

$$\langle Q \rangle = \int QP(\{J\}) dJ. \tag{C.3}$$

The order parameter is denoted by

$$
\begin{aligned}
q = \langle \langle \hat{S}_i \rangle^2_{\{J\}} \rangle &= \lim_{n \to 0} \langle \hat{S}_i^\alpha \hat{S}_i^\beta \rangle_{\alpha \neq \beta} \\
&= \lim_{n \to 0} \left\langle \mathrm{Tr}\, \hat{S}_i^\alpha \hat{S}_i^\beta \exp \left(-\beta \sum_{k=1}^{n} \hat{H}^{(k)} \right) \right\rangle ,
\end{aligned} \tag{C.4}
$$

where $\hat{S}_i^\alpha$ is spin and $\langle \hat{S}_i^\alpha \hat{S}_i^\beta \rangle = \langle \mathrm{Tr}\, \hat{S}_i^\alpha \hat{S}_i^\beta \exp(-\beta \sum_{k=1}^{n} \hat{H}^{(k)}) \rangle$. For convenience, the following quasi free energy is introduced

$$
f_n(m, q) = (-k_B T / nN) \ln \Phi_n, \tag{C.5}
$$

where m is a magnetization and Φ_n is the partition function defined as

$$
\begin{aligned}
\Phi_n = \mathrm{Tr} \left\langle \prod_{k=1}^{n} \exp \left[-\beta \hat{H}^{(k)} \right] \right\rangle \delta \left(\sum_{i,\alpha} \langle \hat{S}_i^\alpha \rangle - mnN \right) \\
\times \delta \left(\sum_{i,\alpha \neq \beta} \langle \hat{S}_i^\alpha \hat{S}_i^\beta \rangle - \frac{n(n-1)N}{2} q \right) .
\end{aligned} \tag{C.6}
$$

The true free energy is investigated by minimizing $f_n(m, q)$

$$
\frac{\partial}{\partial m} f_n(m, q) = 0, \frac{\partial}{\partial q} f_n(m, q) = 0. \tag{C.7}
$$

In the limit $n \to 0$, the free energy is calculated.

In general, the quasi free energy for Eq. (C.5) is expanded in the form

$$
\begin{aligned}
f_n(m, q) = F_0 + (A_n m^2 + B_n m^4 + ...) + (C_n q^2 + D_n q^4 + ...) \\
+ (E_n q m^2 + ...),
\end{aligned} \tag{C.8}
$$

where F_0 is constant and A_n, B_n, C_n, D_n, E_n are function of n, T. This form m^2, q^2, qm^2 results from Eq. (C.6). For example, when Hamiltonian $\hat{H}^{(k)} = \sum_{i,j} \hat{S}_i^\alpha \hat{S}_j^\beta$, Φ_n is written as

$$
\begin{aligned}
\Phi_n &= \left\langle \prod_{k=1}^{n} \exp \left[-\beta \left(\sum_{i,\alpha=\beta} \hat{S}_i^\alpha \hat{S}_i^\alpha + \sum_{i,\alpha \neq \beta} \hat{S}_i^\alpha \hat{S}_i^\beta \right) \right] \right\rangle \delta \left(\sum_{i,\alpha} \langle \hat{S}_i^\alpha \rangle - mnN \right) \\
&\quad \times \delta \left(\sum_{i,\alpha \neq \beta} \langle \hat{S}_i^\alpha \hat{S}_i^\beta \rangle - \frac{n(n-1)N}{2} q \right) \\
&= \left\langle \prod_{k=1}^{n} \exp \left[-\beta ((mnN)^2 + n(n-1)Nq/2) \right] \right\rangle .
\end{aligned}
$$

Thus, $f_n(m,q) \propto m^2, q^2, qm^2$. Considering a magnetic field H, the true free energy is derived by minimizing $f_n(m,q) - hm$ where $h = \mu_B H$ and μ_B is a Bohr magneton. They differentiate $f_n(m,q) - hm$ with respect to m:

$$\frac{\partial f_n(m,q) - hm}{\partial m} = 0, \tag{C.9}$$

$$2m(A_n + E_n q + ...) + 4B_n m^3 + ... = h. \tag{C.10}$$

In $q = 0$, the system is equivalent to quantum spin systems. Thus, the relation between h and m is written by

$$\frac{\partial f(m)}{\partial m} = h, \tag{C.11}$$

$$2mA_n + 4B_n m^3 + ... = h. \tag{C.12}$$

C.2 Case of XXZ chain

For XXZ chain, the transformation between a magnetization m and magnetic field h is written by Legendre transformation. First, we define two Hamiltonian as

$$\hat{\mathscr{H}} = J \sum_{j}^{N} (\hat{S}_j^x \hat{S}_{j+1}^x + \hat{S}_j^y \hat{S}_{j+1}^y + \Delta \hat{S}_j^z \hat{S}_{j+1}^z), \tag{C.13}$$

$$\hat{\mathscr{H}}' = J \sum_{j}^{N} (\hat{S}_j^x \hat{S}_{j+1}^x + \hat{S}_j^y \hat{S}_{j+1}^y + \Delta \hat{S}_j^z \hat{S}_{j+1}^z) - h \sum_{j=1}^{N} \hat{S}_j^z, \tag{C.14}$$

where $\hat{S}_j^x, \hat{S}_j^y, \hat{S}_j^z$ is the jth site spin operator in the x, y, z direction and h is a magnetic field. The lowest energy of $\hat{\mathscr{H}}$ and $\hat{\mathscr{H}}'$ are given by f and $g = f - hm$ where m is a magnetization, f is function of m, and g is function of h.

Next, we relate m to h by Legendre transformation. From the transformation, f and g are related in the following way

$$\begin{aligned} dg &= df - hdm - mdh \\ &= \frac{\partial f}{\partial m} dm - hdm - mdh \\ &= \left(\frac{\partial f}{\partial m} - h \right) dm - mdh. \end{aligned}$$

And then, considering $\frac{\partial f}{\partial m} = h$, we obtain

$$dg = -mdh. \tag{C.15}$$

As g is a function of h, dg is written as follows

$$dg = \left(\frac{\partial g}{\partial h}\right)_m dh. \tag{C.16}$$

Comparing Eq. (C.15) with Eq. (C.16), we obtain

$$\left(\frac{\partial g}{\partial h}\right)_m = -m. \tag{C.17}$$

Thus, f and g satisfies

$$\frac{\partial f}{\partial m} = h, \tag{C.18}$$

$$\left(\frac{\partial g}{\partial h}\right)_m = -m. \tag{C.19}$$

Under the Eq. (C.18) and Eq. (C.19), the Hamiltonian (C.13) is equivalent to the Hamiltonian (C.14). This mean that a magnetization m and magnetic field h are exchanged.

C.3 Nonlinear magnetic susceptibility

A nonlinear magnetic susceptibility is used for a spin–glass study [36] and is related to the high-order differentials such as a magnetic susceptibility χ for Eq. (3.8), fourth derivative A for Eq. (3.9), and third derivative D for Eq. (6.2). The nonlinear magnetic susceptibility χ_{nl} is defined as

$$\chi_{nl} = -\frac{1}{6}\frac{\partial^3 m}{\partial h^3}|_{h=0} \tag{C.20}$$

$$h = \frac{\partial \epsilon(m)}{\partial m} \tag{C.21}$$

where $\epsilon(m)$ is a free energy, m is a magnetization, and h is a magnetic field. χ_{nl} is derived in detail. First, we consider the second derivative of m with respect to

h:

$$\begin{aligned}
\frac{\partial^2 m}{\partial h^2} &= \frac{\partial}{\partial h}\frac{\partial m}{\partial h} \\
&= \frac{\partial}{\partial h}\left(\frac{\partial^2 \epsilon(m)}{\partial m^2}\right)^{-1} \\
&= \frac{\partial m}{\partial h}\frac{\partial}{\partial m}\left(\frac{\partial^2 \epsilon(m)}{\partial m^2}\right)^{-1} \\
&= \frac{\partial m}{\partial h}\left[-\left(\frac{\partial^2 \epsilon(m)}{\partial m^2}\right)^{-2} \times \frac{\partial^3 \epsilon(m)}{\partial m^3}\right] \\
&= -\left(\frac{\partial^2 \epsilon(m)}{\partial m^2}\right)^{-3} \times \frac{\partial^3 \epsilon(m)}{\partial m^3}. \qquad \text{(C.22)}
\end{aligned}$$

Next, we derive χ_{nl} from Eq. (C.22) as follows

$$\begin{aligned}
\chi_{nl} &= -\frac{1}{6}\frac{\partial^3 m}{\partial h^3} \\
&= \frac{1}{6}\frac{\partial m}{\partial h}\frac{\partial}{\partial m}\left[\left(\frac{\partial^2 \epsilon(m)}{\partial m^2}\right)^{-3} \times \frac{\partial^3 \epsilon(m)}{\partial m^3}\right] \\
&= \frac{1}{6}\left(\frac{\partial^2 \epsilon(m)}{\partial m^2}\right)^{-1}\left[-3\left(\frac{\partial^2 \epsilon(m)}{\partial m^2}\right)^{-4}\left(\frac{\partial^3 \epsilon(m)}{\partial m^3}\right)^{2} + \left(\frac{\partial^2 \epsilon(m)}{\partial m^2}\right)^{-3}\frac{\partial^4 \epsilon(m)}{\partial m^4}\right] \\
&= \frac{1}{6}\left[-3\left(\frac{\partial^2 \epsilon(m)}{\partial m^2}\right)^{-5}\left(\frac{\partial^3 \epsilon(m)}{\partial m^3}\right)^{2} + \left(\frac{\partial^2 \epsilon(m)}{\partial m^2}\right)^{-4}\frac{\partial^4 \epsilon(m)}{\partial m^4}\right] \\
&= -\frac{1}{2}\chi^5 D^2 + \frac{1}{6}\chi^4 A, \qquad \text{(C.23)}
\end{aligned}$$

where $\chi^{-1} = \frac{\partial^2 \epsilon(m)}{\partial m^2}$, $D = \frac{\partial^3 \epsilon(m)}{\partial m^3}$, and $A = \frac{\partial^4 \epsilon(m)}{\partial m^4}$. Therefore, χ_{nl} is derived by using χ, A, and D.

Appendix D

Conformal field theory

In this chapter, we introduce the basics of conformal field theory (CFT).

D.1 Conformal algebra for d dimension

We consider the d dimension. In the coordinate transformations $x \to x'$, the metric $g_{\mu\nu} = \eta_{\mu\nu}$ where $\eta_{\mu\nu}$ is the metric of a flat space is transformed in the form

$$g'_{\mu\nu}(x') = \Omega(x) g_{\alpha\beta}(x), \tag{D.1}$$

$$\Omega(x) = \frac{\partial x^\alpha}{\partial x'^\mu}\frac{\partial x^\beta}{\partial x'^\nu}, \tag{D.2}$$

where $\Omega(x)$ is a scale factor. The conformal transformation is defined as Eq. (D.1) and Eq. (D.2). This transformation leaves the angle $\theta = \boldsymbol{v} \cdot \boldsymbol{w}/\sqrt{v^2 w^2}$ between the two vectors $\boldsymbol{v}, \boldsymbol{w}$ invariant.($\boldsymbol{u} \cdot \boldsymbol{v} = g_{\mu\nu} u^\mu v^\nu$) To verify this, we consider the conformal transformation for $\cos\theta$:

$$\begin{aligned}\cos\theta = \frac{\boldsymbol{u} \cdot \boldsymbol{v}}{|\boldsymbol{u}||\boldsymbol{v}|} &= \frac{g_{\mu\nu} u^\mu v^\nu}{\sqrt{g_{\mu\nu} u^\mu u^\nu}\sqrt{g_{\mu\nu} v^\mu v^\nu}} \\ \to \frac{\Omega(x) g_{\mu\nu} u^\mu v^\nu}{\sqrt{\Omega(x) g_{\mu\nu} u^\mu u^\nu}\sqrt{\Omega(x) g_{\mu\nu} v^\mu v^\nu}} &= \frac{g_{\mu\nu} u^\mu v^\nu}{\sqrt{g_{\mu\nu} u^\mu u^\nu}\sqrt{g_{\mu\nu} v^\mu v^\nu}} = \cos\theta.\end{aligned}$$

Thus, the conformal transformation leaves θ invariant. Under the infinitesimal coordinate transformation $x^\mu \to x'^\mu = x^\mu + \epsilon^\mu(x)$, the line element $ds^2 =$

$g_{\mu\nu}\mathrm{d}x^\mu \mathrm{d}x^\nu$ is transformed as

$$\begin{aligned}
ds'^2 &= g'_{\mu\nu}(x')\mathrm{d}x'^\mu \mathrm{d}x'^\nu \\
&= g_{\mu\nu}(x)\mathrm{d}(x^\mu + \epsilon^\mu(x))\mathrm{d}(x^\nu + \epsilon^\nu(x)) \\
&= g_{\mu\nu}\mathrm{d}x^\mu \mathrm{d}x^\nu + g_{\mu\nu}\mathrm{d}x^\mu \frac{\partial \epsilon^\nu(x)}{\partial x^\alpha}\mathrm{d}x^\alpha + g_{\mu\nu}\frac{\partial \epsilon^\mu(x)}{\partial x^\beta}\mathrm{d}x^\beta \mathrm{d}x^\nu + \mathcal{O}(\epsilon^2(x)) \\
&\simeq ds^2 + g_{\mu\alpha}\mathrm{d}x^\mu \partial_\nu \epsilon^\alpha(x)\mathrm{d}x^\nu + g_{\beta\nu}\partial_\mu \epsilon^\beta(x)\mathrm{d}x^\mu \mathrm{d}x^\nu \\
&= ds^2 + (\partial_\nu \epsilon_\mu(x) + \partial_\mu \epsilon_\nu(x))\mathrm{d}x^\mu \mathrm{d}x^\nu,
\end{aligned}$$

where $g'_{\mu\nu}(x') = g_{\mu\nu}(x) = \eta_{\mu\nu}$. To satisfy Eq. (D.1) and Eq. (D.2), $\partial_\nu \epsilon_\mu + \partial_\mu \epsilon_\nu$ must be proportional to $\eta_{\mu\nu}$

$$\partial_\nu \epsilon_\mu + \partial_\mu \epsilon_\nu = A(x)\eta_{\mu\nu}, \tag{D.3}$$

where $A(x)$ is an arbitrary function. Multiplying both sides of Eq. (D.3) by $\eta^{\mu\nu}$, we obtain

$$\eta^{\mu\nu}(\partial_\nu \epsilon_\mu + \partial_\mu \epsilon_\nu) = A(x)\eta^{\mu\nu}\eta_{\mu\nu},$$

where $\eta^{\mu\nu}\eta_{\mu\nu}$ is the sum of the diagonal components of the identity matrix in d dimension. $A(x)$ is derived in the form

$$\begin{aligned}
2\partial_\mu \epsilon^\mu &= A(x)d \\
A(x) &= \frac{2}{d}\partial_\mu \epsilon^\mu.
\end{aligned}$$

Thus, Eq. (D.3) is written as

$$\partial_\nu \epsilon_\mu + \partial_\mu \epsilon_\nu = \frac{2}{d}(\partial_\rho \epsilon^\rho)\eta_{\mu\nu}. \tag{D.4}$$

The infinitesimal coordinate transformation means a conformal transformation as $\Omega(x) = 1 + \frac{2}{d}(\partial_\rho \epsilon^\rho)$. $\epsilon(x)$ that satisfies Eq. (D.4) is called "killing vector" to metric $g_{\mu\nu}$ and becomes a generator of the infinitesimal conformal transformation. Differentiate Eq. (D.4), we obtain

$$\begin{aligned}
\partial_\beta \partial^\nu(\partial_\mu \epsilon_\nu + \partial_\nu \epsilon_\mu) &= \frac{2}{d}\partial_\beta \partial^\nu(\partial \cdot \epsilon)\eta_{\mu\nu} \\
\partial_\beta \partial_\mu(\partial \cdot \epsilon) + (\partial \cdot \partial)\partial_\beta \epsilon_\mu &= \frac{2}{d}\partial_\beta \partial_\mu(\partial \cdot \epsilon).
\end{aligned} \tag{D.5}$$

where $\partial \cdot \epsilon = \partial_\alpha \epsilon^\alpha = \partial^\alpha \epsilon_\alpha$ and $\partial \cdot \partial = \partial_\alpha \partial^\alpha = \partial^\alpha \partial_\alpha$. For $\beta \leftrightarrow \mu$, the equation is

$$\partial_\mu \partial_\beta(\partial \cdot \epsilon) + (\partial \cdot \partial)\partial_\mu \epsilon_\beta = \frac{2}{d}\partial_\mu \partial_\beta(\partial \cdot \epsilon). \tag{D.6}$$

Adding Eq. (D.5) and Eq. (D.6), we obtain

$$2\partial_\mu\partial_\beta(\partial\cdot\epsilon)+(\partial\cdot\partial)(\partial_\mu\epsilon_\beta+\partial_\beta\epsilon_\mu)=\frac{4}{d}\partial_\mu\partial_\beta(\partial\cdot\epsilon). \tag{D.7}$$

By multiplying Eq. (D.7) by $\eta^{\mu\beta}$ and using (D.4), we obtain

$$\begin{aligned}2\eta^{\mu\beta}\partial_\mu\partial_\beta(\partial\cdot\epsilon)+\frac{2}{d}(\partial\cdot\partial)(\partial\cdot\epsilon)\eta^{\mu\beta}\eta_{\mu\beta}&=\frac{4}{d}\eta^{\mu\beta}\partial_\mu\partial_\beta(\partial\cdot\epsilon)\\ 2(\partial\cdot\partial)(\partial\cdot\epsilon)+2(\partial\cdot\partial)(\partial\cdot\epsilon)&=\frac{4}{d}(\partial\cdot\partial)(\partial\cdot\epsilon)\\ (d-1)(\partial\cdot\partial)(\partial\cdot\epsilon)&=0. \end{aligned} \tag{D.8}$$

As a result, the differential equation with respect to ϵ is derived. If $d=1$, ϵ is an arbitrary function. Thus, we exclude $d=1$. Furthermore, from Eq. (D.4) and Eq. (D.7), we obtain

$$2\partial_\mu\partial_\beta(\partial\cdot\epsilon)+\frac{2}{d}(\partial\cdot\partial)(\partial\cdot\epsilon)\eta_{\mu\beta}=\frac{4}{d}\partial_\mu\partial_\beta(\partial\cdot\epsilon).$$

From the perspective of Eq. (D.8), as $(\partial\cdot\partial)(\partial\cdot\epsilon)=0$, the above relation is

$$\left(1-\frac{2}{d}\right)\partial_\mu\partial_\beta(\partial\cdot\epsilon)=0. \tag{D.9}$$

This relation is applied for $d>2$.

The conformal transformation includes various transformations. For instance,

$$\begin{cases}\epsilon^\mu(x)=a^\mu(a^\mu \text{ is constant})\rightarrow \text{translation}\\ \epsilon^\mu(x)=\omega^\mu_\nu x^\nu(\omega^\mu_\nu=-\omega^\nu_\mu)\rightarrow \text{rotation}\\ \epsilon^\mu(x)=\lambda x^\mu(\lambda \text{ is constant})\rightarrow \text{scale}\\ \epsilon^\mu(x)=a^\mu x^2-2x^\mu a\cdot x\rightarrow \text{special conformal}\end{cases}$$

These relations form conformal transformation group for d dimensions and are the same type as $SO(d,2)$ that is the group of rotation around the origin for d dimensions.

D.2 Conformal algebra in $d=2$ dimension

For $d=2$, Eq. (D.4) is transformed as

$$\partial_1\epsilon^1=\partial_2\epsilon^2, \tag{D.10}$$
$$\partial_1\epsilon^2=-\partial_2\epsilon^1, \tag{D.11}$$

where $\epsilon(z) \equiv \epsilon^1 + i\epsilon^2$ and $\overline{\epsilon}(\overline{z}) \equiv \epsilon^1 - i\epsilon^2$ in the complex coordinates $z \equiv x^1 + ix^2$ and $\overline{z} \equiv x^1 - ix^2$. The above relations are same as Cauchy-Riemann equation by introducing the complex coordinates. Thus, the conformal transformations in two dimensions are

$$z \to f(z), \overline{z} \to \overline{f}(\overline{z}), \tag{D.12}$$

$$\partial_{\overline{z}} f(z) = 0, \partial_z \overline{f}(\overline{z}) = 0, \tag{D.13}$$

where $\partial_z \equiv \frac{\partial}{\partial z}$, $\partial_{\overline{z}} \equiv \frac{\partial}{\partial \overline{z}}$, and $f(z)$,$\overline{f}(\overline{z})$ are regular analytic function. $\partial_z, \partial_{\overline{z}}$ are defined as

$$\partial_z \equiv \frac{1}{2}(\partial_x - i\partial_y), \tag{D.14}$$

$$\partial_{\overline{z}} \equiv \frac{1}{2}(\partial_x + i\partial_y). \tag{D.15}$$

This definition is derived from the total derivative of function f;

$$\begin{aligned}
\mathrm{d}f &= \frac{\partial f}{\partial x}\mathrm{d}x + \frac{\partial f}{\partial y}\mathrm{d}y \\
&= \frac{\partial f}{\partial x}\frac{1}{2}(\mathrm{d}z + \mathrm{d}\overline{z}) + \frac{\partial f}{\partial x}\frac{1}{2}(\mathrm{d}z - \mathrm{d}\overline{z}) \\
&= \mathrm{d}z\frac{1}{2}\left(\frac{\partial}{\partial x} - i\frac{\partial}{\partial y}\right) f + \mathrm{d}\overline{z}\frac{1}{2}\left(\frac{\partial}{\partial x} + i\frac{\partial}{\partial y}\right) f \\
&= \frac{\partial f}{\partial z}\mathrm{d}z + \frac{\partial f}{\partial \overline{z}}\mathrm{d}\overline{z}.
\end{aligned}$$

In $f(z) = \epsilon(z)$, Eq. (D.13) are verified:

$$\begin{aligned}
\partial_{\overline{z}} f(z) &= \left(\frac{\partial}{\partial x^1} + i\frac{\partial}{\partial x^2}\right)(\epsilon^1 + i\epsilon^2) \\
&= \frac{\partial \epsilon^1}{\partial x^1} - \frac{\partial \epsilon^2}{\partial x^2} + i\frac{\partial \epsilon^1}{\partial x^2} + i\frac{\partial \epsilon^2}{\partial x^1} \\
&= 0. \quad (\partial_1\epsilon^1 = \partial_2\epsilon^2, \partial_1\epsilon^2 = -\partial_2\epsilon^1)
\end{aligned}$$

Similarly, $\partial_z \overline{f}(\overline{z}) = 0$. In addition, we consider the line element ds^2 in the complex coordinates.

$$ds^2 = (dx^1)^2 + (dx^2)^2 = (dx^1 + idx^2)(dx^1 - idx^2) = dzd\overline{z}.$$

Considering the transformation $z \to w = w(z), \overline{z} \to \overline{w} = \overline{w}(\overline{z})$, the line element is written as following

$$ds^2 \to ds'^2 = dwd\overline{w} = \frac{\partial w}{\partial z}dz\frac{\partial \overline{w}}{\partial \overline{z}}d\overline{z} = \left|\frac{\partial w}{\partial z}\right|^2 ds^2. \tag{D.16}$$

Thus, from Eq. (D.16), the transformations in a complex field show a conformal transformation. To calculate the commutation relations, we take for the basis in the form

$$z \to z' = z + \epsilon(z), \overline{z} \to \overline{z}' = \overline{z} + \overline{\epsilon}(\overline{z}),$$

where $\epsilon(z) = -\sum_n \epsilon_n z^{n+1}$ and $\overline{\epsilon}(\overline{z}) = -\sum_n \epsilon_n \overline{z}^{m+1}$. The corresponding generators are given by

$$l_n = -z^{n+1}\partial_z, \bar{l}_n = -\overline{z}^{n+1}\partial_{\overline{z}}, \quad (n \in \mathbf{Z}) \tag{D.17}$$

where $\mathbf{Z}$ is a whole set of integers. These generators satisfy

$$[l_m, l_n] = (m-n)l_{m+n}, [\bar{l}_m, \bar{l}_n] = (m-n)\bar{l}_{m+n}. \quad (m, n \in \mathbf{Z}) \tag{D.18}$$

l_m and $\bar{l}_n$ commute: $[l_m, \bar{l}_n] = 0$. The proof of $[l_m, l_n] = (m-n)l_{m+n}$ is shown in the following way

$$\begin{aligned}
[l_m, l_n] &= [-z^{m+1}\partial_z, -z^{n+1}\partial_z] \\
&= z^{m+n+2}[\partial_z, \partial_z] + (-z^{m+1})[\partial_z, -z^{n+1}]\partial_z + (-z^{n+1})[-z^{m+1}, \partial_z]\partial_z \\
&+ [z^{m+1}, z^{n+1}]\partial_z\partial_z \\
&= (-z^{m+1})[(n+1)(-z^n) + z^{n+1}\partial_z]\partial_z + (-z^{n+1}) \\
&\times [(m+1)(-z^m) + z^{m+1}\partial_z]\partial_z \\
&= (m-n)z^{n+m+1}\partial_z \\
&= (m-n)l_{m+n}.
\end{aligned}$$

Similarly, $[\bar{l}_m, \bar{l}_n] = (m-n)\bar{l}_{m+n}$ is proved. We call Eq. (D.18) the local conformal transformation.

In contrast, on a Riemann sphere, holomorphic (regular analytic) conformal transformations are given by the vector fields $v(z)$ defined as

$$v(z) = -\sum_n a_n l_n = \sum_n a_n z^{n+1}\partial_z.$$

We then consider the behavior of $v(z)$ to z. In $z \to 0$, $v(z) \neq \infty$ when $a_n \neq 0$ and $n \geq -1$. In $z \to \infty$, we carry out the transformation $z = -1/w$

$$\begin{aligned}
v(z) &= \sum_n a_n \left(-\frac{1}{w}\right)^{n+1} \frac{\partial w}{\partial z}\frac{\partial}{\partial w} = \sum_n a_n \left(-\frac{1}{w}\right)^{n+1} w^2\partial_w \\
&= \sum_n a_n \left(-\frac{1}{w}\right)^{n-1} \partial_w.
\end{aligned}$$

As $w \to 0$, $v(z) \neq \infty$ allows $a_n \neq 0$ and $n \leq 1$. Therefore, the conformal transformations of $a_n l_n$ are defined for $n = 0, \pm 1$. When a conformal transformations are the projection to the Riemann sphere from another Riemann sphere, the conformal transformations are called a global conformal transformations. The global transformation is defined as

$$z \to \frac{az+b}{cz+d}. \quad (ad - bc \neq 0) \tag{D.19}$$

This relation is related to coefficient of Möbius transformation:

$$SL(2,C) \simeq SO(2,2) = \begin{pmatrix} a & b \\ c & d \end{pmatrix}. \quad (ad - bc = 1) \tag{D.20}$$

D.3 Primary field

In a conformal transformation $z \to z'$, a primary field $\Phi(z, \overline{z})$ transforms as

$$\Phi(z,\overline{z}) = \Phi'(z',\overline{z}') \left(\frac{dz'}{dz}\right)^h \left(\frac{d\overline{z}'}{d\overline{z}}\right)^{\overline{h}}, \tag{D.21}$$

where h and $\overline{h}$ are called "conformal weight(dimension)" and are independent. When h and $\overline{h}$ are considered to be an integer, the primary field is an extension of a tensor field in two dimensions.

First, we consider the rotation around the origin:

$$z \to z' = e^{i\theta} z, \overline{z} \to \overline{z}' = e^{-i\theta}\overline{z}. \tag{D.22}$$

From Eq. (D.21), the primary field is written as

$$\Phi(z,\overline{z}) = \Phi'(z',\overline{z}') e^{i\theta(h-\overline{h})}. \tag{D.23}$$

This equation shows that the field $\Phi(z, \overline{z})$ has a spin $S = h - \overline{h}$, as the representation of $SO(2) = U(1)$ is equal to $e^{iS\theta}$.

Next, we consider the scale transformation:

$$z \to z' = \lambda z, \overline{z} \to \overline{z}' = \lambda \overline{z}. \quad (\lambda > 0) \tag{D.24}$$

Subsequently, the primary field transforms as

$$\Phi(z,\overline{z}) = \Phi'(z',\overline{z}') \lambda^{h+\overline{h}}. \tag{D.25}$$

This equation shows that the scaling dimension which indicates the critical exponent of $\Phi(z, \overline{z})$ is $\Delta = h + \overline{h}$. These equations give the relation of $h, \overline{h}$:

$$h + \overline{h} = \Delta, h - \overline{h} = S. \tag{D.26}$$

Finally, we consider a general transformation $z \to F(z)$. The primary field transforms as

$$\Phi'(z,\overline{z}) \equiv \Phi(F(z),\overline{F(z)}) \left(\frac{dF}{dz}\right)^h \overline{\left(\frac{dF}{dz}\right)}^{\overline{h}}. \tag{D.27}$$

Under the infinitesimal transformation $F(z) = z + \epsilon f(z) + \mathcal{O}(\epsilon^2)$ where ϵ is small and $f(z)$ is complex function, Eq. (D.27) is written as

$$\begin{aligned}\Phi'(z,\overline{z}) &\equiv \Phi(z+\epsilon f(z), \overline{\epsilon}\overline{f}(\overline{z}))(1+\epsilon f'(z))^h\overline{(1+\epsilon f'(z))}^{\overline{h}} + \mathcal{O}(\epsilon^2) \\ &= \Phi(z,\overline{z}) + \epsilon f(z)\frac{\partial\Phi}{\partial z} + {}_hC_1\epsilon f'(z)\Phi + \epsilon\overline{f(z)}\frac{\partial\Phi}{\partial\overline{z}} + {}_{\overline{h}}C_1\epsilon\overline{f'(z)}\Phi + \mathcal{O}(\epsilon^2) \\ &= \Phi(z,\overline{z}) + \epsilon\delta_f\Phi(z,\overline{z}) + \epsilon\overline{\delta}_f\Phi(z,\overline{z}) + \mathcal{O}(\epsilon^2),\end{aligned}$$

where $\delta_f = f(z)\frac{\partial}{\partial z} + h\epsilon f'(z), \overline{\delta}_f = \overline{f(z)}\frac{\partial}{\partial\overline{z}} + \overline{h}\overline{f'(z)}$. The transformation means that the primary field is divided into z, h and $\overline{z}, \overline{h}$.

$$\Phi_{h,\overline{h}}(z,\overline{z}) = \Phi_h(z)\overline{\Phi}_{\overline{h}}(\overline{z}). \tag{D.28}$$

If $f(z) = z^{n+1}$, $\delta_f\Phi(z,\overline{z})$ and $\overline{\delta}_f\Phi(z,\overline{z})$ are given by

$$\delta_f\Phi(z,\overline{z}) \equiv z^{n+1}\frac{\partial\Phi(z,\overline{z})}{\partial z} + h(n+1)z^n\Phi(z,\overline{z}), \tag{D.29}$$

$$\overline{\delta}_f\Phi(z,\overline{z}) \equiv z^{n+1}\frac{\partial\Phi(z,\overline{z})}{\partial\overline{z}} + \overline{h}(n+1)\overline{z}^n\Phi(z,\overline{z}). \tag{D.30}$$

In particular, Eq. (D.29) and Eq. (D.30) with $n = \pm 1, 0$ are called as a quasi-primary field.

References

[1] H.A. Bethe. Zur theorie der metalle. Zeitschrift für Physik, 71:205–226, 1931.

[2] F.D.M. Haldane. Phys. Rev. Lett, 50:1153, 1983.

[3] J. des Cloizeaux and M. Gaudin. J. Math. Phys, 7:1384, 1966.

[4] H. Nakano and T. Sakai. J. Phys.:Conf. Series, 868:012006, 2017.

[5] H. Nakano and T. Sakai. J. Phys. Soc. Jpn, 80:053704, 2011.

[6] T. Sakai and H. Nakano. Physica B, 536:85, 2018.

[7] T. Sakai and H. Nakano. J. Phys.: Conf. Series, 969:012127, 2018.

[8] M. Matsumoto et al. Phys. Rev. B, 65:014407, 2011.

[9] R.B. Griffiths. Phys. Rev, 133:A768, 1964.

[10] L. Hulthen. Ark. Mat. Astr. Fys, 26A:No. 11, 1938.

[11] J. des Cloizeaux and I. J. Pearson. Phys. Rev, 128:2131, 1962.

[12] C.N. Yang and C.P. Yang. Phys. Rev, 151:258, 1966.

[13] C.N. Yang and C.P. Yang. Phys. Rev, 150:327, 1966.

[14] S. Lukyanov. Nucl. Phys. B, 522:533, 1998.

[15] T. Sakai and M. Takahashi. Phys. Rev. B, 43:13383, 1991.

[16] A. Kitazawa and K. Nomura. J. Phys. Soc. Jpn, 66:3944, 1997.

[17] L.P. Kadanoff. Ann. Phys, 120:39, 1979.

[18] K. Nomura. J. Phys. A: Math. Gen, 28:5451, 1995.

[19] A.W.W. Ludwig, J.L. Cardy. Nucl. Phys. B, 285:687, 1987.

[20] K. Nomura. Phys. Rev. B, 48:16814, 1993.

[21] H. Nishimori. http://hdl.handle.net/2433/94584, 1991.

[22] M. Kawamura, K. Yoshimi, T. Misawa, Y. Yamaji, S. Todo, and N. Kawashima. Comp. Phys. Commun, 217:180–192, 2017.

[23] M. Takahashi. Thermodynamics of One-Dimensional Solvable Models. Cambridge University Press, 1999.

[24] A. Luther and I. Peschel. Phys. Rev. B, 12:3908, 1975.

[25] C.N. Yang and C.P. Yang. Phys. Rev, 150:321, 1966.

[26] N. Goldenfeld. Lectures on phase transition and the renormalization group. Westview Press, Boulder, 1992.

[27] L.D. Faddeev. Développments Récents en Théorie des champs et Mécanique Statistique. North-Holland, Amsterdam, 1983.

[28] E. Lieb, T. Schultz, and D. Mattis. ANNALS OF PHYSICS, 16:401–466, 1961.

[29] I. Affleck and E.H. Lieb. Lett. Math. Phys, 12:57, 1986.

[30] M. Takahashi and T. Sakai. J. Phys. Soc. Jpn, 60:760–763, 1991.

[31] E.H. Lieb and W. Liniger. Phys. Rev, 130:1605, 1963.

[32] C.N. Yang and C.P. Yang. J. Math. Phys, 10:1115, 1969.

[33] K. Kawano and M. Takahashi. J. Phys. Soc. Jpn, 64:4331–4344, 1995.

[34] S. Eggert, I. Affleck, and M. Takahashi. Phys. Rev. Lett, 73:332, 1994.

[35] P. Ginsparg. "Applied Conformal Field Theory" in Les Houches, Session XLIX, 1988, Fields, Strings and Critical Phenomena edited by E. Brézin, J. Zinn-Justin. North-Holland, Amsterdam, 1989.

[36] M. Suzuki. Prog. Theor. Phys, 58:1151, 1977.

[37] J.L. Cardy. Conformal invariance, in Phase transitions, volume 11 of by C. Domb and J.L. Lebowitz. Academic Press, 1987.

[38] S.K. Yang. Nucl. Phys. B, 285:183, 1987.

[39] J. Cardy. Scaling and Renormalization in Statistical Physics. Cambridge University Press, 1996.

[40] H.W.J. Blöte, J.L. Cardy, and M.P. Nightingale. Phys. Rev. Lett, 56:742, 1986.

[41] I. Affleck. Phys. Rev. Lett, 56:746, 1986.

[42] J.L. Cardy. J. Phys. A, 19:L385, 1984.